

# First determination of $f_+(0)|V_{us}|$ from a combined analysis of $\tau \rightarrow K\pi\nu_\tau$ decay and $\pi K$ scattering with constraints from $K_{\ell 3}$ decays

---

**Véronique Bernard<sup>a</sup>**

<sup>a</sup>*Groupe de Physique Théorique, Institut de Physique Nucléaire, CNRS/IN2P3,  
Université Paris-Sud 11, 91406 Orsay, France*

*E-mail:* [bernard@ipno.in2p3.fr](mailto:bernard@ipno.in2p3.fr)

**ABSTRACT:** We perform a combined analysis of  $\tau \rightarrow K\pi\nu_\tau$  decay and  $\pi K$  scattering with constraints from  $K_{\ell 3}$  data using a  $N/D$  approach that fulfills requirements from unitarity and analyticity. We obtain a good fit of the  $I = 1/2$   $\pi K$  amplitude in the  $P$  wave using the LASS data above the elastic region while in this region data are generated via Monte Carlo using the FOCUS results based on  $D_{\ell 4}$  decay. The spectrum and branching ratio of  $\tau \rightarrow K\pi\nu_\tau$  constrained by  $K_{\ell 3}$  decays are also well reproduced leading to  $f_+(0)|V_{us}| = 0.2163 \pm 0.0014$ . Furthermore, we obtain the slope of the vector form factor  $\lambda_+ = (25.56 \pm 0.40) \times 10^{-3}$  while the value of the scalar form factor at the Callan-Treiman point is  $\ln C = 0.2062 \pm 0.0089$ . Given the experimental precision our results are compatible with the Standard Model.

---

## Contents

|          |  |           |
|----------|--|-----------|
| <b>1</b> | <b>Introduction</b>  | <b>1</b>  |
| <b>2</b> | <b><math>\tau \rightarrow K\pi\nu_\tau</math> and <math>K_{\ell 3}</math> decays</b> | <b>3</b>  |
| <b>3</b> | <b>Model</b>   | <b>5</b>  |
| 3.1      | Vector channel   | 5         |
| 3.1.1    | $N/D$ description of $K\pi$ scattering: one channel case                             | 5         |
| 3.1.2    | Resonance contributions to $K\pi$ scattering   | 6         |
| 3.1.3    | Vector form factor   | 9         |
| 3.2      | Dispersive representation of the form factor   | 10        |
| 3.3      | Scalar form factor   | 11        |
| 3.4      | Sum rules  | 13        |
| <b>4</b> | <b>Results</b>   | <b>13</b> |
| 4.1      | Parameters and their order of magnitudes   | 13        |
| 4.2      | $K\pi$ amplitude   | 14        |
| 4.3      | Combined fit   | 16        |
| 4.3.1    | Fit with constraint on $f_+(0) V_{us} $  | 16        |
| 4.3.2    | Role of the constraint on $f_+(0) V_{us} $ and of the curvature of $f_+(s)$ .        | 25        |
| <b>5</b> | <b>Conclusion</b>  | <b>26</b> |

---

## 1 Introduction

One important issue in the test of the Standard Model (SM) as well as in various new physics scenarios is the possible violation of the unitarity of the Cabibbo Kobayashi Maskawa matrix (CKM) as well as the determination of bounds on it. With the present very precise knowledge of the element  $V_{ud} = 0.97425 \pm 0.00022$  from the superallowed  $0^+ \rightarrow 0^+$  nuclear  $\beta$  decays [1, 2] a determination of  $V_{us}$  allows for such a test between the elements of the first row  $|V_{ud}|^2 + |V_{us}|^2 + |V_{ub}|^2 = 1$ .<sup>1</sup> There exists several ways of extracting the matrix element  $V_{us}$ . One of them is the study of leptonic and semileptonic kaon decays. In the latter the combination  $f_+(0)|V_{us}|$  enters, with  $f_+(0)$  the strangeness changing vector form factor at zero momentum transfer. With the progress on the theoretical side in determining the radiative corrections and isospin breaking effects as well as the progress from the lattice community a very precise determination of  $|V_{us}|$  from these decays becomes possible. At present a global analysis including results published by the BNL-E865, KLOE, KTeV, ISTRA+ and NA48 experiments leads to [3]  $f_+(0)|V_{us}| = 0.2163(5)$ .

---

<sup>1</sup>Indeed one can safely neglect the third element which is very small  $|V_{ub}| = (4.15 \pm 0.49) \cdot 10^{-3}$  [1].

Furthermore, it has been advocated in Refs. [4, 5] that the study of  $K_{\ell 3}$  decays in particular offers another possibility to test the SM through the determination of the scalar form factor at the Callan-Treiman (CT) point. Indeed  $SU(N_f) \times SU(N_f)$  low-energy theorems dictate the value of this form factor at that point for  $N_f = 2$  as well as its soft kaon analog for  $N_f = 3$ . Thus a deviation from the value at the CT point, once the corrections  $\Delta_{CT}$  to the theorems are very precisely known would be a sign of physics beyond the SM such as right-handed quark couplings to the  $W$  boson or charged Higgs effects (see for example the discussion in [6]). This has triggered a renewal of activity on the experimental side. Three collaborations, NA48 [7], KLOE [8] and KTeV [9] reanalyzed their data on  $K_{\mu 3}^0$  decays so as to extract the value of the scalar form factor at the CT point. With the current experimental precision, NA48 has a  $4.5\sigma$  deviation from the SM while KLOE/KTeV show a good/marginal agreement with the SM. However, the NA48/2 experiment has recently released preliminary results for the form factors for both  $K_{e3}^\pm$  and  $K_{\mu 3}^\pm$  decays which are now consistent with the results from the two other collaborations [10]. In fact, there seems to be some inconsistencies in the older measurement from NA48 for  $K_L$  [11].

Additional information on the quantity  $f_+(0)|V_{us}|$  as well as on the scalar form factor can be gained from the dominant Cabibbo-suppressed  $\tau$  decay  $\tau \rightarrow K\pi\nu_\tau$ . It has been measured by BaBar [12] and Belle [13] and studied by several groups [14]–[19]. It was shown that adding constraints from  $K_{\ell 3}$  yielded a more precise result for the low-energy part of the vector form factor [18]. However, at present this decay has never been used to determine  $f_+(0)|V_{us}|$ , rather this quantity was taken as input and a determination of the mass and width of the resonances present in the spectrum was performed. As noticed recently [20] one can extract this quantity from  $\tau$  decays and this is one of the goals of this work using the experimental constraints from the publicly available Belle spectrum of  $\tau \rightarrow K_S\pi^-\nu_\tau$  decay.

Information on the mass and width of the resonances contributing to the form factors can also be obtained from other experiments, e.g. production ones as well as the semileptonic decay  $D_{\ell 4}$  [21, 22]. Furthermore Watson’s theorem relates the phase of the scalar and vector form factors to the phases of  $K\pi$  scattering in the elastic region. Another aim of this paper is thus to gather all the information one has from these decays as well as from production experiments following [16]<sup>2</sup> in order to get a very precise determination of the normalized strangeness changing vector and scalar form factors in a way as model independent as possible. This is mandatory for a very precise knowledge of  $|V_{us}|$  as well as in searches for beyond-SM CP violation in  $\tau \rightarrow K\pi\nu_\tau$ . These are pursued by CLEO [23] and more recently Belle and BaBar [24, 25].

Here we concentrate on the region  $\sqrt{s} < \sqrt{s}_{\text{cut}} \sim 1.65$  GeV. Indeed from threshold to  $s_{\text{cut}}$  inelasticities in the  $P$  waves are mostly saturated by the  $K^*(892)$  and the  $K^*(1410)$  and to some extent by the  $K^*(1680)$ . This allows us to model the vector form factor in a rather simple way in that region using a coupled channel  $N/D$  method. This method fulfilling

---

<sup>2</sup>In this reference LASS data on  $K\pi$  scattering were fitted in order to determine all the parameters related to the resonances appearing in the determination of  $\tau$  decays. However in that work, the quantity  $f_+(0)|V_{us}|$  was an input parameter.

the requirement of analyticity and unitarity the result can be matched to a three-times subtracted dispersion relation assuming that the vector form factor has no zeros. This will allow us to make direct contact with other works since these relations are extensively used in the literature, for comparable issues as discussed here let us mention the descriptions of the  $\pi\pi$  form factor in [26] and of the  $K\pi$  ones in [17, 18]. In the latter the inelasticities coming from the  $K^*\pi$  channel as well as the sum rules obeyed by the slope and the curvature which will be discussed here, were not taken into account. The scalar form factor, in its turn, is described using a twice-subtracted dispersion relation following [4, 5]. Since the energy region considered here is larger than the one considered in these works, one subtraction more could help taming the effect of the unknown high energy region, in the spirit of what is done for the vector form factor. However it is not so helpful since a sum rule is constraining the additional parameter in the expression of the form factor. Thus contrary to our previous work [20] we will perform the fit to the  $\tau$  data with the twice-subtracted dispersion relation and study the dependence of our results on the parametrization of the high energy region. We will also for comparison study the extensively used scalar form factor determined from a coupled channel method [27, 28]. For a recent related work on scalar form factors in semileptonic B-decays, see Ref. [29].

In section 2, we define the quantities needed in our analysis. Then in section 3 we detail our model. First we briefly summarize the  $N/D$  method in the one channel case and then generalize it to the two coupled channel one for  $\pi K$  scattering. We then describe the vector and scalar form factors and establish the sum rules they should fulfill. We discuss the parameters of the fit especially their expected order of magnitude. Results of several joined fits to  $\tau \rightarrow K\pi\nu_\tau$  and  $\pi K$  scattering data constrained by  $K_{\ell 3}$  decays are given in section 4. We finally discuss our determination of  $f_+(0)|V_{us}|$  and the role played by constraining its value in the combined fit as well as the value of the curvature of the vector form factor and conclude.

## 2 $\tau \rightarrow K\pi\nu_\tau$ and $K_{\ell 3}$ decays

The differential decay distribution of the decay  $\tau \rightarrow \bar{K}^0\pi^-\nu_\tau$  reads

$$\begin{aligned} \frac{d\Gamma_{K\pi}(s)}{d\sqrt{s}} &= \frac{G_F^2 m_\tau^5}{48\pi^3} S_{EW}^\tau |V_{us}|^2 |f_+(0)|^2 I_K^\tau(s) , \\ I_K^\tau(s) &= \frac{1}{m_\tau^2} \left(1 - \frac{s}{m_\tau^2}\right)^2 \left[ \left(1 + \frac{2s}{m_\tau^2}\right) \frac{q_{K\pi}^3(s)}{s} |\bar{f}_+(s)|^2 + \frac{3q_{K\pi}(s)(m_K^2 - m_\pi^2)^2}{4s^2} |\bar{f}_0(s)|^2 \right] , \end{aligned} \quad (2.1)$$

where  $s = (p_\pi + p_K)^2$ ,  $G_F$  is the Fermi constant,  $S_{EW}^\tau = 1.0201(3)$  the short distance electroweak correction [30] and  $q_{K\pi}$  the kaon momentum in the rest frame of the hadronic system,

$$q_{K\pi}(s) = \frac{\lambda^{1/2}(s, m_\pi^2, m_K^2)}{2\sqrt{s}} , \quad (2.2)$$

with the Källén's function  $\lambda(s, m_\pi^2, m_K^2) = (s - (m_K + m_\pi)^2)(s - (m_K - m_\pi)^2)$ .  $I_K^\tau(s)$  probes the energy-dependence of the strangeness changing  $K\pi$  form factors normalized to

one at the origin,  $\bar{f}_{+,0}(s) \equiv f_{+,0}(s)/f_{+,0}(0)$ . The vector form factor is defined as

$$\langle K^0(p_K) | \bar{u} \gamma^\mu s | \pi^-(p_\pi) \rangle = f_+(t) (p_K + p_\pi)^\mu + f_-(t) (p_K - p_\pi)^\mu, \quad (2.3)$$

with  $t = (p_K - p_\pi)^2$ , while the scalar form factor  $f_0(t)$  is the combination

$$f_0(t) = f_+(t) + \frac{t}{M_K^2 - M_\pi^2} f_-(t). \quad (2.4)$$

Eq. (2.1) does not take into account the long distance electromagnetic and strong isospin-breaking corrections. These corrections introduce small  $s$ -dependent factors multiplying both the terms proportional to the vector and the scalar form factors as well as an additional interference term between the two form factors not written here. Once the distribution is integrated they lead to corrections which have been recently evaluated [31] and are of the order of a few percent. Clearly a very precise determination of  $|V_{us}|$  requires a very accurate determination of all the quantities on the RHS of Eq. (2.1) (as well as a very accurate measurement of  $\Gamma_{K\pi}$ ), however at the level of accuracy of the data neglecting these corrections is perfectly legitimate.

In order to determine  $f_+(0)|V_{us}|$  an observable of interest is the branching ratio which is obtained by integrating the decay spectrum

$$B_{K\pi} = \frac{G_F^2 m_\tau^5}{96\pi^3} S_{ew} \tau_\tau |f_+(0)V_{us}|^2 I_K^\tau, \quad (2.5)$$

with  $I_K^\tau$  the phase space integral

$$I_K^\tau = \int_{(m_K+m_\pi)^2}^{m_\tau^2} I_K^\tau(s) \frac{ds}{\sqrt{s}}, \quad (2.6)$$

and  $\tau_\tau$  the tau life time. Up to very recently the experimental value from the Belle collaboration was [13],

$$B_{exp} \equiv B[\tau^- \rightarrow \nu_\tau K_S \pi^-] = (0.404 \pm 0.002 \text{ (stat)} \pm 0.013 \text{ (syst)}) \% \quad (2.7)$$

A value consistent with this study was reported in [32], while the new update is about  $1\sigma$  higher with an improved accuracy [33]

$$B_{exp} \equiv B[\tau^- \rightarrow \nu_\tau K_S \pi^-] = (0.416 \pm 0.001 \text{ (stat)} \pm 0.008 \text{ (syst)}) \% \quad (2.8)$$

For BaBar results see [34].

Similar expressions as given for  $\tau \rightarrow K\pi\nu_\tau$  hold for  $K_{\ell 3}$  decays, the hadronic matrix elements for these two processes being related by crossing. In that case  $S_{EW}^{K_{\ell 3}} = 1.0232(3)$  [35]. Long distance electromagnetic and strong isospin breaking corrections are again small  $\delta_{EM}^{K_{\ell 3}} = (0.495 \pm 0.110)\%$  for the neutral channel,  $\delta_{EM}^{K_{\ell 3}} = (0.050 \pm 0.125)\%$  for the charged channel and  $\delta_{SU(2)}^{K_{\ell 3}} = 0.029(4)$ , [36, 37].

Here we are interested in the region from threshold to  $\sqrt{s} \sim 1.65$  GeV which, as already stated, is dominated by two resonances the  $K^*(892)$  and the  $K^*(1410)$ , the latter decaying predominantly into  $K^*\pi$ . It is thus legitimate to use a two channel approach to describe

$K\pi$  scattering as well as  $\tau$  decays in that region, the two most relevant channels being  $K\pi$  and  $K^*\pi$ . These channels will be labelled

$$1 \longrightarrow K\pi, \quad 2 \longrightarrow K^*\pi. \quad (2.9)$$

This implies that in a coupled channel description one has not only to consider the strangeness changing vector form factor, Eq. (2.3), but also the vector current matrix element

$$\langle K^{*+}(p_V, \lambda) | \bar{u} \gamma_\mu s | \pi^0(p_\pi) \rangle = \epsilon_{\mu\nu\alpha\beta} e^{*\nu}(\lambda) p_V^\alpha p_\pi^\beta H_2(t). \quad (2.10)$$

Consequently, as in [16], the model generates predictions for  $\tau$  decaying into  $K^*\pi$  via the vector current, the energy distribution of the decay width being

$$\frac{d\Gamma_{K^*\pi}(s)}{d\sqrt{s}} = \frac{G_F^2 m_\tau^3}{32\pi^3} q_{K^*\pi}^3(s) |V_{us}|^2 \left(1 - \frac{s}{m_\tau^2}\right) \left(1 + \frac{2s}{m_\tau^2}\right) |H_2(s)|^2. \quad (2.11)$$

One has information, though not very precise, on the integrated rate from Aleph,  $R^{\text{Aleph}}(\tau \rightarrow K^*(1410)\nu_\tau \rightarrow K\pi\pi\nu_\tau) = (1.4_{-0.9}^{+1.3} \pm 0.0) \times 10^{-3}$  where the first uncertainty comes from the fit to the  $K\pi$  invariant mass, while the second uncertainty arises from the possibility for the  $K^*(1410)$  to decay into  $K\eta$  [38].

### 3 Model

#### 3.1 Vector channel

Unitarity relates the imaginary part of the vector form factor to the  $K\pi$  scattering amplitude in the  $J=1$  channel. We will thus first describe this scattering in a two channel approach using the  $N/D$  method.

##### 3.1.1 $N/D$ description of $K\pi$ scattering: one channel case

Let us consider the partial wave amplitude with total angular momentum one, and more specifically the quantity  $T^1(s)$  which has the proper behavior at threshold, i.e. it vanishes as  $q_{K\pi}^2(s)$ .  $T^1(s)$  has two kind of cuts, the right-hand cut required by unitarity

$$(\text{Im}T^1(s))^{-1} = -q_{K\pi}^2(s)\rho(s), \quad \rho(s) = \frac{q_{K\pi}(s)}{8\pi\sqrt{s}}\theta(s - s_{\text{th}}), \quad (3.1)$$

and the unphysical ones from crossing symmetry. In our case the latter comprise a left hand cut and a circular one in the complex  $|s|$  plane for  $|s| = m_K^2 - m_\pi^2$ . A standard way to determine the T-matrix using the knowledge of these cuts is the  $N/D$  method, where the partial wave is expressed as the ratio

$$T^1(s) = \frac{N(s)}{D(s)}, \quad (3.2)$$

with  $D(s)$  encoding the right-hand cut and  $N(s)$  the unphysical ones. In the phenomenological application used here, it should be safe to neglect the latter as a first approximation. Indeed, it has been shown in [39] that considering them in a perturbative manner should

be realistic in the physical region. Also, tadpoles and loops in crossed channel are soft contributions which will be reabsorbed in some low energy constants. Hence in the zeroth order approximation,  $N(s) = 1$  and all the zeros of  $T^1$  will be poles of  $D(s)$ . The most general structure of the T-matrix with the unphysical cuts neglected thus reads, see [40] for more details:

$$T(s) = \frac{1}{D(s)},$$

$$D(s) = -\frac{(s-s_0)^2}{\pi} \int_{s_{\text{th}}}^{\infty} ds' \frac{q_{K\pi}^2(s') \rho(s')}{(s'-s)(s'-s_0-i\epsilon)^2} + c_0 + c_1 s + \sum_i \frac{R_i}{s-s_i}. \quad (3.3)$$

The poles in  $D(s)$  referred to as CDD poles [41] either can be linked to particles (resonances/bound states) with the same quantum numbers as those of the partial wave amplitude or enter to ensure the presence of zeros of the amplitude required by the underlying theory such as Adler zeros.

Splitting the two constants  $c_0$  and  $c_1$  into a leading and a subleading part (we will discuss in more detail how we define leading and subleading in the next section)

$$c_i = c_i^{\text{lead}} + c_i^{\text{sub}}, \quad (3.4)$$

one can write

$$T^{\text{lead}}(s) = \left( c_0^{\text{lead}} + c_1^{\text{lead}} s + \sum_i \frac{R_i}{s-s_i} \right)^{-1}$$

$$g(s) = c_0^{\text{sub}} + c_1^{\text{sub}} s - \frac{(s-s_0)^2}{\pi} \int_{s_{\text{th}}}^{\infty} ds' \frac{q_{K\pi}^2(s') \rho(s')}{(s'-s)(s'-s_0-i\epsilon)^2}. \quad (3.5)$$

One thus finally gets the basic equation for the T-matrix:

$$T(s) = \left( 1/T^{\text{lead}}(s) + g(s) \right)^{-1}. \quad (3.6)$$

Writing  $K^{-1} = (T^{\text{lead}})^{-1} + \text{Re } g$ , one recovers the well known K-matrix approach.

### 3.1.2 Resonance contributions to $K\pi$ scattering

Before generalizing to the two channel case, let us discuss what we mean by leading and subleading order. In the region of interest here, pions and kaons are not the only relevant degrees of freedom. Resonances have to be taken into account explicitly. It thus seems natural to use the framework of Resonance Chiral Theory (R $\chi$ PT) [42, 43]. This scheme developed in the mesonic sector incorporates Goldstone bosons and resonance fields within a Lagrangian approach. It is based on Large  $N_c$  arguments and uses short distant constraints and OPE results (note that we do not discuss the problems with a consistent power counting for loop graphs in such an approach here). At present, most applications have been done at tree level but some issues related to the next-to-leading order which involves complicated one loop calculations in a non-renormalizable theory have already been addressed, for

references see [44]. The Resonance Chiral Theory Lagrangian is given by a sum of two terms

$$\mathcal{L}_{\text{R}\chi\text{PT}} = \mathcal{L}_{\chi\text{PT}} + \mathcal{L}_R , \quad (3.7)$$

where  $\mathcal{L}_{\chi\text{PT}}$  is the Chiral Perturbation Theory ( $\chi\text{PT}$ ) Lagrangian up to a given chiral order but with Low Energy Constants (LECs) different from the ones when no resonance terms are present, whereas  $\mathcal{L}^R$  is the part of the Lagrangian describing the resonances. Consequently, our leading order constants  $c_i^{\text{lead}}$  will contain the contributions from this Lagrangian at tree level *i.e.* the leading large  $N_c$  contributions while the  $1/N_c$  ones (loops plus subleading tree level contributions) will be given by the  $c_i^{\text{sub}}$  terms.

Let us concentrate on the resonance part. There are two resonances below  $\sqrt{s} \sim 1.65$  GeV: the  $K^*(892)$  and the  $K^*(1410)$ . However the  $K^*(1680)$  is rather close and is rather broad, thus it can affect the description of the close-by region. We will thus consider these three resonances here. The experimental decay branching ratios for the  $K^*(1410)$  and the  $K^*(1680)$  [1] are

$$\begin{aligned} K^*(1410) : & \quad (6.6 \pm 1)\% (K\pi), \quad > 40\% (95\% \text{ confidence level}) (K^*\pi) \\ K^*(1680) : & \quad (38.7 \pm 2.5)\% (K\pi), \quad (29.9^{+2.2}_{-4.7})\% (K^*\pi), \quad (31.4^{+4.7}_{-2.1})\% (K\rho). \end{aligned} \quad (3.8)$$

Since for simplicity we do not take into account the  $K\rho$  channel, the last branching ratio of the  $K^*(1680)$  cannot be obtained in our model. Thus our description of this resonance is not completely accurate but this should not affect our results in a significant way.

There are two ways of describing spin-one particles in  $\text{R}\chi\text{PT}$  (for a general review on vector meson chiral Lagrangians, see [45]). Following Ref. [16], we will work in the vector formalism in which the nonet of the light vector mesons are encoded in a matrix  $V_\mu$ . The chiral Lagrangian is given by [46]

$$\mathcal{L}_R = \sum_{i=1}^3 \mathcal{L}_K^{(i)} + \mathcal{L}_V^{(i)} + \mathcal{L}_\sigma^{(i)} , \quad (3.9)$$

with

$$\begin{aligned} \mathcal{L}_K^{(1)} &= \frac{-1}{4} \text{tr} (V_{\mu\nu} V^{\mu\nu} - 2M_V^2 V_\mu V^\mu) , \\ \mathcal{L}_V^{(1)} &= \frac{-i}{2\sqrt{2}} g_V(1) \text{tr} (V_{\mu\nu} [u_\mu, u_\nu]) , \\ \mathcal{L}_\sigma^{(1)} &= \frac{1}{2} \sigma_V(1) \epsilon^{\mu\nu\rho\sigma} \text{tr} (V_\mu \{u_\nu, V_{\rho\sigma}\}) . \end{aligned} \quad (3.10)$$

Here,  $V_{\mu\nu} = \nabla_\mu V_\nu - \nabla_\nu V_\mu$  and  $u_\mu$  describes the light pseudoscalars. Similarly, the Lagrangian for an excited vector resonance  $V_\mu^{(n)}$  reads ( $n \neq 1$ )

$$\begin{aligned} \mathcal{L}_V^{(n)} &= \frac{-i}{2\sqrt{2}} g_V(n) \text{tr} (V_{\mu\nu}^{(n)} [u_\mu, u_\nu]) , \\ \mathcal{L}_\sigma^{(n)} &= \frac{1}{2} \sigma_V(n) \epsilon^{\mu\nu\rho\sigma} \text{tr} (V_\mu^{(n)} \{u_\nu, V_{\rho\sigma}\}) . \end{aligned} \quad (3.11)$$

We have written explicitly the terms which do not involve the quark mass matrix and, therefore, have exact  $SU(3)$  flavor symmetry. This is sufficient for our purposes.



Using Eqs. (3.10), (3.11) the resonance contribution to the  $T$ -matrix has been obtained in Ref. [16]. It can be written in a compact form displaying the usual resonance structure:

$$T_{ij}^{\text{res}} = \sum_n \frac{g(n,i)g(n,j)}{M_n^2 - s} , \quad (3.12)$$

with

$$\begin{aligned} g(n,1) &= \frac{g_V(n)}{\sqrt{16\pi}} \left( \frac{\sqrt{s}}{F_\pi} \right)^2 , \\ g(n,2) &= \frac{\sigma_V(n)}{\sqrt{16\pi}} \frac{\sqrt{2s}}{F_\pi} (1 + \delta_{n1}) , \end{aligned} \quad (3.13)$$

and the sum runs in our case over the three resonances considered here.

Implementing 2-channel unitarity using the  $N/D$  method discussed previously the leading order  $T^{\text{lead}}$ -matrix and  $g$  are now  $2 \times 2$  matrices (see Eq. 2.9 for the labelling of the channels). The former has the following general form

$$T^{\text{lead}} = \begin{pmatrix} a_0 + a_1 s + T_{11}^{\text{res}} & a_4 \sqrt{s} + T_{12}^{\text{res}} \\ a_4 \sqrt{s} + T_{21}^{\text{res}} & a_2 + a_3 s + T_{22}^{\text{res}} \end{pmatrix} , \quad (3.14)$$

In the  $1 \rightarrow 1$  channel  $a_0$  and  $a_1$  come from the tree level contributions of the  $\chi$ PT Lagrangian, Eq. (3.7). We refrain from giving their expressions here but we will comment more on them in section 4. For the other channels, the  $a_i$  are unknown coefficients.

In our effective theory approach  $g$  is the diagonal matrix representing the fundamental bubble one-loop-integral illustrated in the blue box of Fig. 1. It is given by

$$g(s) = - \begin{pmatrix} 48\pi (F_\pi^2 H_{K\pi}(s) + l_{K\pi}) & 0 \\ 0 & 48\pi (F_\pi^2 H_{K^*\pi}(s) + l_{K^*\pi}) \end{pmatrix} . \quad (3.15)$$

where  $H_{ab}(s)$  is the well-known scale-independent function in  $\chi$ PT, see Ref. [47]

$$H_{ab}(s) = \frac{1}{F_\pi^2} (s M_{ab}^r(s) - L_{ab}(s)) + \frac{2}{3F_\pi^2} L_{ab}^r s , \quad (3.16)$$

$l_{ab}$  and  $L_{ab}^r$  contain the polynomial part of the loops and the subleading contributions from  $\mathcal{L}_{\chi\text{PT}}$ , Eq. (3.7). Note that  $L_{ab}^r$  is a scale-dependent quantity which cancels the scale-dependence from the combination  $s M_{ab}^r(s) - L_{ab}(s)$ . As it is written,  $g(s)$  respects the dispersive integral, Eq. (3.5). Indeed, it has the same imaginary part and thus can differ only by polynomial terms. These can be absorbed into the parameters  $l_{ab}$  and  $L_{ab}^r$ .

The  $K$ -matrix approach used in Ref. [16] can be obtained from these expressions defining  $K^{-1} = (T^{\text{lead}})^{-1}$  and keeping only the imaginary part of  $g$ . Similarly to this approach, the  $S$ -matrix defined by

$$S = 1 + 2gT , \quad (3.17)$$

is unitary.

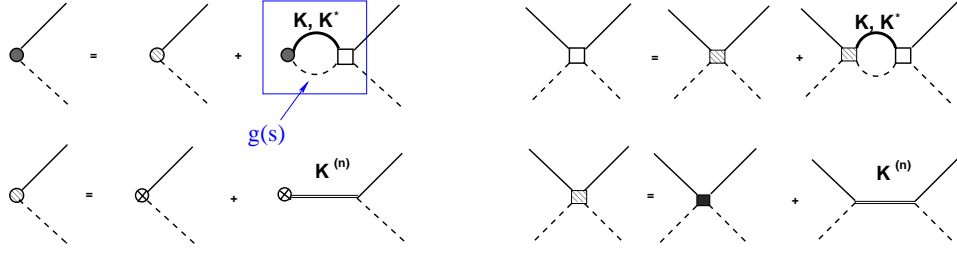


**Figure 1.** Representation of the  $T_{11}$  matrix element (right panel) and of the vector form factor (left panel). The full/dashed external lines represent the kaon/pion respectively. The double line stands for one of the three resonances while the thick line in the loops stands for the kaon or the  $K^*$ . The fundamental bubble which appears in the blue box on the left panel is described by  $g(s)$ , Eq. (3.15).

### 3.1.3 Vector form factor

Following Ref. [16], we will focus on one of the spatial components of the vector current and go to the center-of-mass (CM) frame of the meson pair. This allows to project onto  $f_+(s)$  and use unitarity requirements to derive an equation for the vector form factors in a similar way to what has been done first for scalar form factors [48] and then for example in [49]. For completeness, we will summarize the argument here. Defining the matrix of the vector form factors

$$\Gamma(s) = \begin{pmatrix} f_+(s) \\ \sqrt{s} H_2(s) \end{pmatrix}, \quad (3.18)$$

unitarity implies the following relation between  $\Gamma(s)$  and the  $J = 1$   $T$  matrix, see Eq. (3.6)

$$\text{Im}\Gamma(s) = T(s) \frac{2Q^3(s)}{\sqrt{s}} \Gamma^*(s), \quad (3.19)$$

with

$$Q(s) = \begin{pmatrix} q_{K\pi}(s) & 0 \\ 0 & q_{K^*\pi}(s) \end{pmatrix}.$$

where  $q_{K^*\pi}(s)$  is defined in a similar way as  $q_{K\pi}(s)$ , Eq. (2.2) but with the kaon mass replaced by the  $K^*$  mass. Substituting in the previous equation  $\text{Im}\Gamma(s)$  by  $(\Gamma(s) - \Gamma^*(s))/(2i)$  and  $T(s)$  by its expression, Eq. (3.6), one has

$$\Gamma(s) = \left[ I + T^{\text{lead}}(s) g(s) \right]^{-1} \left( I + T^{\text{lead}}(s) g(s) + T^{\text{lead}}(s) \frac{4iQ^3(s)}{\sqrt{s}} \right) \Gamma^*(s). \quad (3.20)$$

Taking into account that  $T^{\text{lead}}$  is real and that

$$g^*(s) = g(s) + 4i \frac{Q^3(s)}{\sqrt{s}}, \quad (3.21)$$

one can write

$$\left(I + T^{\text{lead}}(s) g(s)\right) \Gamma(s) = \left(I + T^{\text{lead}}(s) g^*(s)\right) \Gamma^*(s) , \quad (3.22)$$

which implies that the quantity  $(I + T^{\text{lead}}(s) g(s)) \Gamma(s)$  has no cuts since the only one which appears in  $g(s)$  and  $\Gamma(s)$ , the right-hand cut, is removed. Therefore one can finally write

$$\Gamma(s) = \left[I + T^{\text{lead}}(s) g(s)\right]^{-1} \mathcal{R}(s) , \quad (3.23)$$

where  $\mathcal{R}(s)$  is a matrix of real functions free of any singularity.

We will fix  $\mathcal{R}(s)$  by requiring matching to R $\chi$ PT obtaining

$$\mathcal{R}(s) = \begin{pmatrix} \left(h_1 + \sqrt{16\pi} \sum_n g(n, 1) F_n s \left(\frac{1}{M_n^2 - s} + \frac{1}{s}\right)\right) \\ \sqrt{s} h_2 + \sqrt{16\pi} \sum_n g(n, 2) F_n \frac{s}{M_n^2 - s} \end{pmatrix} ,$$

with  $F_n$  defined by

$$\mathcal{L} = -\frac{F_n}{2\sqrt{2}} \langle V_{\mu\nu}^{(n)} f_+^{\mu\nu} \rangle , \quad (3.24)$$

and  $h_1$  and  $h_2$  are such that the quantities on the right-hand-side of Eq. (3.23) give the proper normalization of the form factors at  $s = 0$ . In the expression of the first row of  $\mathcal{R}(s)$  we have added the term  $1/s$  to the resonance contribution. It has indeed been shown in [43] that such a term is required for consistency with QCD when using a vector field formulation to describe the spin-1 resonances.

Keeping only one channel and one resonance and using the relation from R $\chi$ PT

$$F_{K^*} g_V M_{K^*}^2 / F_\pi^2 = 1 \quad (3.25)$$

with  $F_{K^*} \equiv F_1$ , Eq. (3.23) reduces to the formula used in Ref. [17]

$$f_+^{K\pi}(s) = \frac{m_{K^*}^2}{m_{K^*}^2 - s - \kappa H_{K\pi}(s)} , \quad (3.26)$$

with  $\kappa$  a dimensionful constant.<sup>3</sup>

### 3.2 Dispersive representation of the form factor

The function  $\Gamma(s)$ , Eq. (3.18) is clearly only a good description of the form factors up to  $\sqrt{s} \sim 1.65$  GeV, in particular it does not have the proper behaviour at infinity. This is completely sufficient for our purpose. However, since unitarity and the analyticity properties are fulfilled, the vector form factor can be rewritten as a dispersion relation that employs the phase extracted from Eq. (3.18) supplemented by some parametrization of the phase at higher energy. In order to compare with other works as well as to check our calculation we will match our vector form factor to a three times subtracted dispersion relation

---

<sup>3</sup> In the last equation we expanded the coupling of the resonance to  $K\pi$ , which is proportional to  $s$ , around the off-shellness of the resonance using  $s = m_{K^*}^2 + \delta s$  [16].

following [17], the number of subtractions allowing in principle to tame the dependence on the high energy part of the phase. Assuming that the form factor has no zeros one can write [17]:

$$f_+^{K\pi}(s) = f_+(0) \exp \left\{ \alpha_1 \frac{s}{M_{\pi^-}^2} + \frac{1}{2} \alpha_2 \frac{s^2}{M_{\pi^-}^4} + \frac{s^3}{\pi} \int_{s_{K\pi}}^{\infty} ds' \frac{\delta_1^{K\pi}(s')}{(s')^3 (s' - s - i\epsilon)} \right\}, \quad (3.27)$$

where the phase of the form factor  $\delta_1^{K\pi}(s)$  in the region from threshold to  $\sqrt{s} = 1.6$  GeV is obtained from Eq. (3.23). One has

$$\delta_1^{K\pi}(s) = \text{atan}(\text{Im}\Gamma_{11}(s)/\text{Re}\Gamma_{11}(s)) \quad \text{for } (M_K + M_\pi)^2 < s < (1.6 \text{ GeV})^2. \quad (3.28)$$

At higher energy the phase is unknown. However the knowledge of the asymptotic behaviour of the form factor [50] for large  $s$  allows to model it in a very rough way. Indeed the phase  $\delta_1^{K\pi}$  should go to  $\pi$  (modulo  $2\pi$ ) at large  $s$ . Furthermore sum rules have to be fulfilled, see next section. Thus the following simple model for the phase will be used:

$$\delta_1^{K\pi}(s) = n_v \pi \quad \text{for } s > (1.6 \text{ GeV})^2, \quad (3.29)$$

where the quantity  $n_v$  should be such that the sum rules discussed in Sec. 3.4 are satisfied to a good accuracy.  $\alpha_1$  and  $\alpha_2$  in Eq. (3.27) are related to the slope  $\lambda'_+$  and the curvature  $\lambda''_+$  of the form factor as obtained from Eq. (3.23)

$$\alpha_1 = \lambda'_+, \quad \alpha_2 = \lambda''_+ - \lambda'^2_+. \quad (3.30)$$

The formula Eq. (3.27) relies on the assumption that the form factor has no zeros. A technique to find regions on the real axis and in the complex plane where zeros are excluded has been developed and applied in particular to the vector and scalar form factors, see [51] for more discussions. Also the role of zeros in form factors has been discussed in [52].

### 3.3 Scalar form factor

In the scalar case the inelasticities set in later than in the vector case [53, 54]. Therefore, the validity of a single-channel treatment is accordingly extended, and it is thus possible, in our region of interest, to write an expression similar to the one we have just written assuming that the form factor has no zeros but with a simple single-channel expression for the phase. A recent discussion on the presence or absence of zeros in this form factor can be found in [29]. However, in that case, it is more appropriate to use other subtraction points than the ones at zero momentum transfer. One subtraction is done at zero and the two others at the Callan-Treiman point  $\Delta_{K\pi} = M_K^2 - M_\pi^2$ . Indeed the Callan-Treiman low-energy theorem [55] fixes the value of the scalar form factor at that particular point in the  $SU(2) \times SU(2)$  chiral limit

$$f_0(\Delta_{K\pi}) = \frac{F_K^+}{F_\pi^+} + \Delta_{CT}, \quad (3.31)$$

where  $F_{K,\pi}$  are the kaon and pion decay constants, respectively, and  $\Delta_{CT} \sim \mathcal{O}(m_{u,d}/4\pi F_\pi)$  is a small correction which has been computed in the framework of  $\chi$ PT. One thus has

$$f_0^{K\pi}(s) = f_+(0) \exp \left\{ \frac{s}{\Delta_{K\pi}} \left( \ln C + (s - \Delta_{K\pi})\alpha + \tilde{G}(s) \right) \right\} \quad (3.32)$$

with

$$\tilde{G}(s) = \frac{\Delta_{K\pi}s(s - \Delta_{K\pi})}{\pi} \int_{s_{K\pi}}^{\infty} ds' \frac{\delta_0(s')}{s'^2(s' - \Delta_{K\pi})(s' - s - i\epsilon)}, \quad (3.33)$$

and

$$\alpha = \frac{\ln C}{\Delta_{K\pi}} - \frac{\lambda_0}{M_\pi^2}, \quad (3.34)$$

where  $\lambda_0$  is the slope of the scalar form factor and  $\delta_0(s)$  its phase. According to Watson theorem,  $\delta_0$  should coincide in the elastic region ( $s < \Lambda^2$ ) with  $\delta_0^{K\pi}(s)$ , the S-wave  $I=1/2$   $\pi K$  scattering one. Following Refs. [4, 5] one has:

$$\begin{aligned} \delta_0 &= \delta_0^{K\pi}(s) \quad \text{for} \quad (M_K + M_\pi)^2 < s < \Lambda^2 \\ &= n_s \pi \quad \text{for} \quad s > \Lambda^2, \end{aligned} \quad (3.35)$$

where  $\delta_0^{K\pi}(s)$  is taken from the work [56] where a matching of the solution of Roy-Steiner equations with  $K\pi \rightarrow K\pi$ ,  $\pi\pi \rightarrow K\bar{K}$  and  $\pi\pi \rightarrow \pi\pi$  scattering data available at higher energies was performed. We refer the reader to that work where the resulting phase  $\delta_0^{K\pi}(s)$  is discussed. In Eq. (3.35)  $n_s$  can again be estimated such that the sum rules discussed below are satisfied to a good accuracy. One could also think of using independent means to constrain this quantity as for example the QCD sum rules for the strangeness-changing scalar correlation function which allows to relate the strange quark mass to the strange scalar form factor [57]. While this is beyond the scope of this paper, investigation along this line is in progress<sup>4</sup>. The value of  $\Lambda$  will be discussed in Section 4.3.

Since there are sum rules which link the two parameters  $\ln C$  and  $\alpha$  to the high-energy phase we will rather make the fits in what follows with a twice-subtracted relation as in [4, 5] and study the dependence of our results on the high-energy phase. Thus our final expression for the scalar form factor will be

$$f_0^{K\pi}(s) = f_+(0) \exp \left\{ \frac{s}{\Delta_{K\pi}} \left( \ln C + G(s) \right) \right\}, \quad (3.36)$$

with

$$G(s) = \frac{\Delta_{K\pi}(s - \Delta_{K\pi})}{\pi} \int_{s_{K\pi}}^{\infty} ds' \frac{\delta_0(s')}{s'(s' - \Delta_{K\pi})(s' - s - i\epsilon)}, \quad (3.37)$$

and the phase defined in Eq.(3.35).

---

<sup>4</sup>I would like to thank the referee for pointing out this fact to me

### 3.4 Sum rules

As  $t \rightarrow -\infty$ , one expects  $f(t) = \mathcal{O}(1/t)$  [50]. This asymptotic behaviour dictates the following sum rules for the slope and the curvature of the form factors. For the vector form factor one has

$$\lambda'_+ = \frac{m_\pi^2}{\pi} \int_{s_{K\pi}}^{\infty} ds' \frac{\delta_1^{K\pi}(s')}{s'^2}, \quad (3.38)$$

$$\lambda''_+ - \lambda'^2_+ = \frac{2m_\pi^4}{\pi} \int_{s_{K\pi}}^{\infty} ds' \frac{\delta_1^{K\pi}(s')}{s'^3}. \quad (3.39)$$

Similar relations hold for  $\ln C$  and  $\lambda_0$ :

$$\ln C = \frac{\Delta_{K\pi}}{\pi} \int_{s_{K\pi}}^{\infty} ds' \frac{\delta_0^{K\pi}(s')}{s'(s' - \Delta_{K\pi})} \quad (3.40)$$

$$\frac{\ln C}{\Delta_{K\pi}} - \frac{\lambda_0}{M_\pi^2} = \frac{\Delta_{K\pi}}{\pi} \int_{s_{K\pi}}^{\infty} ds' \frac{\delta_0^{K\pi}(s')}{s'^2(s' - \Delta_{K\pi})} \quad (3.41)$$

The sum rule for  $\ln C$  has been studied in Ref. [5].

## 4 Results

### 4.1 Parameters and their order of magnitudes

One has 18 parameters to be fitted in the scattering case: 9 of them corresponds to the mass and the two coupling constants  $g_V^n$  and  $\sigma_V^n$  of the three resonances  $K^*(892)$ ,  $K^*(1410)$  and  $K^*(1680)$ . The remaining parameters are the five  $a_i$ 's and the four  $l_{ab}$ ,  $L_{ab}^r$  with  $(ab) = K\pi$  and  $K^*\pi$ , respectively. In the case of  $\tau$  decay 7 parameters more have to be fitted,  $\ln C$ ,  $I_k^\tau$ ,  $f_+(0)|V_{us}|$ ,  $H_2(0)/f_+(0)$  and  $F_n/f_+(0)$ , the couplings of the three resonances to the vector source. Note that these couplings as well as  $H_2(0)$  are divided by the value of the vector form factor at zero momentum transfer since this quantity cannot be determined as it always enters combined with  $V_{us}$ . Furthermore since our vector form factor is only valid up to  $\sim 1.65$  GeV we will not integrate  $I_k^\tau(s)$  up to  $m_\tau$  but rather use  $I_k^\tau$  as a parameter of the fit. We will also allow the parameter  $n_s$  in Eq. (3.35) to be free in order to study the dependence of our results on the high energy region.

Typical order of magnitudes for these parameters are:

- within  $\chi$ PT one has at leading order  $a_0 = 1/(32\pi F(3)^2)$  where  $F(3)$  is the pion decay constant in the SU(3) chiral limit. Usually  $F(3)$  is traded with  $F_\pi$ , the difference being of higher orders and thus  $a_0 = 1.16 \text{ GeV}^{-2}$ . However there are some indications from several studies that possibly significative differences of patterns exist between the  $N_f = 2$  and  $N_f = 3$  chiral limits [58]-[62]. Such differences can be interpreted as a paramagnetic suppression of chiral order parameters when the number of massless flavors in the theory increases, in relation with the role of  $\bar{s}s$  vacuum pairs in chiral dynamics. Consequently

$F(3)$  could be smaller than  $F_\pi$  in a non negligible way, a ratio  $F_\pi/F(3) \sim 1.3$  being not excluded. We will thus leave  $a_0$  free in the fit, expecting its value in the range  $1.16 - 2.25$ .

- As stated before  $l_{K\pi}$  and  $L_{K\pi}$  contain contributions from the polynomial part of the  $K\eta$ ,  $K\pi$  loops as well as the tadpoles together with some subleading LEC contributions. Typical order of magnitudes for the  $\mathcal{O}(1/N_c)$  LECs in  $\chi$ PT at a scale  $m_\rho$  is  $10^{-4}$ .

- The combination  $a_0 + a_1(m_K + m_\pi)^2$  is related to the  $K\pi$  scattering length  $a_1^{1/2}$ . Indeed expanding the  $T$  matrix at small momentum one has

$$\frac{2}{\sqrt{s}}T = q_{K\pi}^2(a_1^{1/2} + b_1^{1/2}q_{K\pi}^2 + c_1^{1/2}q_{K\pi}^4 + \mathcal{O}(q^6)) \quad (4.1)$$

Some values obtained in the literature for  $a_1^{1/2}$  are summarized in Table 2.

- Based on the extended NJL model:  $g_V^1 \sim 0.08$  and  $\sigma_V^1 \sim 0.25$ .
- As we have seen previously  $F_K^* g_V M_K^2 / f_\pi^2 \sim 1$  in  $R\chi$ PT thus one expects  $F_K^* \sim 10^{-2}/g_V$ , and from our previous estimate  $F_K^* \sim 0.1$ .
- The value of  $H_2(0)$  has been discussed in [16]. In the chiral limit flavor symmetry is exact and  $H_2(0)$  can be related to the radiative width of the charged  $\rho$  meson. Using the experimental value of this width leads to  $H_2(0) = (1.54 \pm 0.08) \text{ GeV}^{-1}$  where the sign was fixed using a vector dominance picture which gives  $H_2(0)$  in terms of the ABJ anomaly. Refining this estimate taking into account the breaking of flavor symmetry the author of Ref. [16] obtains  $H_2(0) \sim (1.41 \pm 0.09 - 65.4a) \text{ GeV}^{-1}$  with  $a$  such that  $|a| < 10^{-2}$ .
- As we discussed in the introduction we will add the constraints from  $K_{\ell 3}$  decays on the values of  $\ln C$ ,  $\lambda'_+$  and  $f_+(0)|V_{us}|$  which are given in Table 2. One more constraint comes from the branching ratio, Eqs. (2.5, 2.7).

## 4.2 $K\pi$ amplitude

In order to determine the parameters which enter the  $T$  matrix we will do a fit to the LASS data [53]. However the data available from this collaboration are given before unfolding the mass resolution [63]. Taking this effect into account affects significantly the central value of the width of the  $K^*(892)$ . Indeed before unfolding the value is 56 MeV to be compared with the 50 MeV result quoted in the literature. However the effect on its mass value should be very small as well as on the data points above 1 GeV.

Thus in the following we will use the LASS data from 1 GeV to 1.65 GeV. However we need the  $I=1/2$  amplitude since our aim is to combine the knowledge from  $K\pi$  scattering with the one from  $\tau$  decay. The LASS data being a combination of the  $I=1/2$  and  $I=3/2$  amplitudes we will correct them using the following parametrization for  $\delta^{I=3/2}$  which is valid above 1 GeV [64]

$$\delta^{I=3/2} = \arctan(\alpha q_{K\pi}^3 / (1 + \beta q_{K\pi}^6)), \quad (4.2)$$

where  $\alpha = -0.101292 \pm 0.02121 \text{ GeV}^{-3/2}$  and  $\beta = 0.331824 \pm 1.668 \text{ GeV}^{-3}$  are obtained from a fit to the Estabrooks data [54].

The data in the elastic region i.e. below 1 GeV can be very well described by the Breit-Wigner form:

$$A(s) = \frac{m_{K^*}^2 \Gamma_{K^*}(m_{K^*}^2)}{s - m_{K^*}^2 + im_{K^*} \Gamma_{K^*}(s)} F_1(s) \quad (4.3)$$

|                     | combined fit $\tau + \pi K$   |                           | Exp.   |
|---------------------|-------------------------------|---------------------------|--|
|                     | $\lambda''_+$ not constrained | $\lambda''_+$ constrained |  |
| $n_s$               | $0.788 \pm 0.258$             | $0.785 \pm 0.194$         |  |
| $\ln C$             | $0.2062 \pm 0.0089$           | $0.2064 \pm 0.0081$       | 0.2004(91)<br>$0.2038 \pm 0.0241$ , $0.1915 \pm 0.0116$<br>$0.1354 \pm 0.0133$ , $0.2084 \pm 0.0134$ |
| $f_+(0) V_{us} $    | $0.2163 \pm 0.0014$           | $0.2163 \pm 0.0012$       | 0.2163(5)  |
| $I_k^\tau$          | $0.485 \pm 0.011$             | $0.485 \pm 0.003$         |  |
| $\overline{F_1}$    | $0.1668 \pm 0.0138$           | $0.1559 \pm 0.000$        | $H_2(0) : 1.41 \pm 0.09 - 65.4a$   |
| $\overline{F_2}$    | $-0.0048 \pm 0.0234$          | $0.0224 \pm 0.001$        |  |
| $\overline{F_3}$    | $-0.0464 \pm 0.0057$          | $-0.0351 \pm 0.0001$      |  |
| $\overline{H_2}(0)$ | $1.46 \pm 0.61$               | $1.52 \pm 0.02$           |  |

|               |                    |                     |                               |                    |                    |
|---------------|--------------------|---------------------|-------------------------------|--------------------|--------------------|
| $M_1$         | $0.898 \pm 0.013$  | $0.909 \pm 0.000$   | $a_0$ [GeV <sup>-2</sup> ]    | $2.190 \pm 0.132$  | 2.270*             |
| $g_V(1)$      | $0.048 \pm 0.006$  | $0.048 \pm 0.000$   | $a_1$ [GeV <sup>-4</sup> ]    | $0.067 \pm 0.180$  | $0.054 \pm 0.009$  |
| $\sigma_V(1)$ | $0.334 \pm 0.067$  | $0.238 \pm 0.001$   | $a_2$ [GeV <sup>-2</sup> ]    | $-0.187 \pm 2.670$ | $-5.807 \pm 0.001$ |
| $M_2$         | $1.292 \pm 0.059$  | $1.314 \pm 0.003$   | $a_3$ [GeV <sup>-4</sup> ]    | $5.122 \pm 1.112$  | $6.348 \pm 0.026$  |
| $g_V(2)$      | $-0.015 \pm 0.006$ | $-0.0137 \pm 0.000$ | $a_4$ [GeV <sup>-3</sup> ]    | $-0.308 \pm 0.609$ | $-0.776 \pm 0.009$ |
| $\sigma_V(2)$ | $0.807 \pm 0.166$  | $0.764 \pm 0.007$   | $l_{K\pi} \times 10^{-3}$     | 0*                 | $0.093 \pm 0.001$  |
| $M_3$         | $1.544 \pm 0.031$  | $1.544 \pm 0.004$   | $L_{K\pi}^r \times 10^{-3}$   | $0.566 \pm 0.141$  | $0.560 \pm 0.009$  |
| $g_V(3)$      | $0.007 \pm 0.002$  | $0.007 \pm 0.000$   | $l_{K^*\pi} \times 10^{-3}$   | $0.037 \pm 0.264$  | $0.511 \pm 0.001$  |
| $\sigma_V(3)$ | $0.433 \pm 0.053$  | $0.406 \pm 0.010$   | $L_{K^*\pi}^r \times 10^{-3}$ | $0.624 \pm 0.574$  | $0.005 \pm 0.003$  |
|               |                    |                     | $\chi^2/\text{d.o.f}$         | 121.26/128         | 120.70/129         |

**Table 1.** Parameters of two combined fits to the  $\tau \rightarrow K\pi\nu_\tau$ , and  $\pi K$  scattering data using some constraints from  $K_{\ell 3}$  decays, see text. In the second column of the three tables the curvature of  $f_+(s)$  is unconstrained while in the third it is forced to be within a given range, Eq. (4.16). A bar on a quantity denotes that the quantity is divided by  $f_+(0)$  while a star on a number indicates that the parameter has been fixed in the fit. The last column of the upper table gives the corresponding experimental results, the first number for  $\ln C$  and the one for  $f_+(0)|V_{us}|$  being from  $K_{\ell 3}$  data taken from the compilation [3] and the numbers on the second and third line for  $\ln C$  are in order from KLOE [8], KTeV [9], NA48 [7] and ISTRA+, see [3]. The experimental number for  $H_2(0)$  is from [16] with  $|a| < 10^{-2}$  where  $a$  is a measure of flavor symmetry breaking. The  $L^r$ 's are evaluated at the scale  $\mu = 0.897$  GeV and  $\Lambda = 1.52$  GeV has been used here. The masses of the resonances are in GeV.



with

$$\Gamma_{K^*}(s) = \Gamma_{K^*}(m_{K^*}^2) r \frac{m_{K^*}}{\sqrt{s}} F_1^2(s), \quad F_1(s) = r B(q_{K\pi}) / B(q_{K\pi}(s = m_{K^*}^2)) \quad (4.4)$$

where  $r = q_{K\pi}/q_{K\pi}(s = m_{K^*}^2)$  and  $B = 1/\sqrt{(1 + r_{BW}^2 q_{K\pi}^2)}$  is the Blatt-Weisskopf damping factor. This form reproduces e.g. the LASS data below 1 GeV [53]. There exists, however, more recent results from the FOCUS collaboration [21] based on the  $D^+ \rightarrow K^- \pi^+ \mu^+ \nu$  decay:

$$M_{K^*(892)} = 895.41 \pm 0.32_{-0.43}^{+0.35} \text{ MeV}, \quad \Gamma_{K^*(892)} = 47.79 \pm 0.86_{-1.06}^{+1.32} \text{ MeV}, \\ r_{BW} = 3.96 \pm 0.54_{-0.90}^{+1.31} \text{ GeV}^{-1}. \quad (4.5)$$

Data for the phase which could in principle be extracted from this decay [65] is not available from this collaboration. We thus generated our own data below  $\sim 1$  GeV via Monte Carlo. A fit of these data leads to  $M_{K^*} = 895.41 \pm 0.68$  MeV,  $\Gamma_{K^*} = 47.80 \pm 1.77$  MeV and  $r_{BW} = 3.91 \pm 1.86$  GeV $^{-1}$  which is a good representation of the FOCUS results.

We can now turn to a combined description of  $\tau$  decays and  $\pi K$  scattering.

### 4.3 Combined fit

The  $\tau \rightarrow K \pi \nu_\tau$  decay has been measured by Belle and BaBar. Here we will fit the Belle spectrum [13]<sup>5</sup>. One has in the  $i$ -th bin

$$N_{\text{events}} = \mathcal{N}_T b_w \frac{1}{\Gamma_\tau B_{K\pi}} \frac{d\Gamma_{K\pi}}{d\sqrt{t}} \quad (4.6)$$

with  $\mathcal{N}_T$  the total number of observed signal events,  $b_w$  the chosen bin-width (in GeV/bin) and  $d\Gamma_{K\pi}/d\sqrt{t}$  the decay spectrum defined in Eq.(2.1).  $\Gamma_\tau$  represents the total decay width of the  $\tau$  lepton and  $B_{K\pi}$  is the total branching fraction, Eq. (2.5). Clearly,  $f_+(0)|V_{us}|$  appears in this formula both in the numerator and in the denominator and thus drops from the ratio, its knowledge being unnecessary for fitting the spectrum.

#### 4.3.1 Fit with constraint on $f_+(0)|V_{us}|$

Table 1 gives the value of the  $\chi^2/\text{d.o.f}$  and of the parameters obtained from a combined fit to  $\tau \rightarrow K \pi \nu_\tau$  and  $\pi K$  scattering data with some constraints from  $K_{\ell 3}$  decays and from the newest value of  $B_{K\pi}$  [33]. We will first discuss the case without constraint on the curvature of the vector form factor. Fig. 2 compares respectively the  $I = 1/2$   $\pi K$  phase and modulus of the amplitude in the  $P$  wave with the corrected LASS data above the elastic region and the data generated from the FOCUS results below. The number of events  $N_{\text{events}}$  from the Belle data and the model is depicted in Fig. 3 as a function of  $\sqrt{s}$ . It is clear from these figures that the combined fit is excellent. This is confirmed by the very good  $\chi^2/\text{d.o.f}$  defined as:

---

<sup>5</sup>We would like to acknowledge D. Epifanov for providing us with the Belle spectrum.

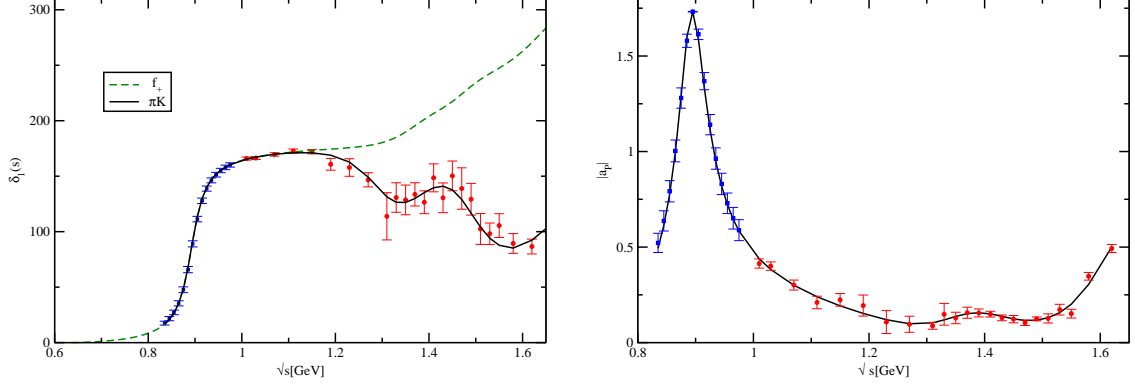


**Figure 2.** Left panel: Phase of the vector form factor (green dashed line) compared to the  $P$  wave  $I = 1/2$   $\pi K$  phase (black solid line). Right panel: Modulus of the  $P$  wave  $I = 1/2$   $\pi K$  amplitude. The blue squares are the data generated via Monte Carlo using the FOCUS results and the red circles are the corrected LASS data, see text.

$$\begin{aligned}
\chi^2 &\equiv \chi_{\text{noct}\lambda''}^2 = \chi_{\text{noctfV}}^2 + \left( \frac{|f_+(0)V_{us}| - |f_+(0)V_{us}|^{\text{exp}}}{\sigma_{|f_+(0)V_{us}|^{\text{exp}}}} \right)^2, \\
\chi_{\text{noctfV}}^2 &= \sum_i \left( \frac{\delta_i - \delta_i^{\text{exp}}}{\sigma_{\delta_i^{\text{exp}}}} \right)^2 + \sum_i \left( \frac{a_i - a_i^{\text{exp}}}{\sigma_{a_i^{\text{exp}}}} \right)^2 + \left( \frac{a_1^{1/2} - a_1^{\text{exp}}}{\sigma_{a_1^{\text{exp}}}} \right)^2 + \sum_i \left( \frac{N_i - N_i^{\text{exp}}}{\sigma_{N_i^{\text{exp}}}} \right)^2 \\
&\quad + \begin{pmatrix} \ln C - \ln C^{K_{\ell 3}} \\ \lambda'_+ - \lambda'_+{}^{K_{\ell 3}} \end{pmatrix}^T V^{-1} \begin{pmatrix} \ln C - \ln C^{K_{\ell 3}} \\ \lambda'_+ - \lambda'_+{}^{K_{\ell 3}} \end{pmatrix} + \left( \frac{B_{K\pi} - B_{K\pi}^{\text{exp}}}{\sigma_{B^{\text{exp}}}} \right)^2 \\
&\quad + \left( \frac{n_s - 0.75}{0.25} \right)^2 + \left( \frac{h_2 - H_2(0)}{0.75} \right)^2
\end{aligned} \tag{4.7}$$

where  $V$  is the covariance matrix and  $\rho(\ln C, \lambda'_+) = -0.33$  [3]. Our fit is performed with 84 points from the Belle data in the energy region from threshold to 1.6 GeV and 39 experimental points  $\delta_i^{\text{exp}}$  for the phase of  $\pi K$  scattering up to 1.66 GeV. Since in the elastic region phase and amplitude are related via a sinus we only fit the amplitude above this region and thus one has only 24 data points  $a_i^{\text{exp}}$  in the second sum. We have constrained  $f_+(0)|V_{us}|$  as  $0.2160 \pm 0.0014$  which corresponds to the error band given by the  $K_{\ell 3}$  data without averaging them but rather taking the smallest/largest value obtained in the various experiments, see discussion below. Furthermore  $B_{K\pi}^{\text{exp}} = 0.416$  and  $\sigma_{B^{\text{exp}}} = 0.008$ , see Eq. (2.7). The former smaller result for  $B_{K\pi}$ , Eq. (2.5) leads to similar results with essentially somewhat smaller values for  $I_k^T$  and the curvature of the vector form factor. We will come back on the constraint on  $n_s$  below. The last constraint takes into account the fact that  $h_2$  is a leading order result and thus should dominate if one expects the series to converge rapidly. The same holds of course for  $h_1$ , but we did not enforce it in the fit. One

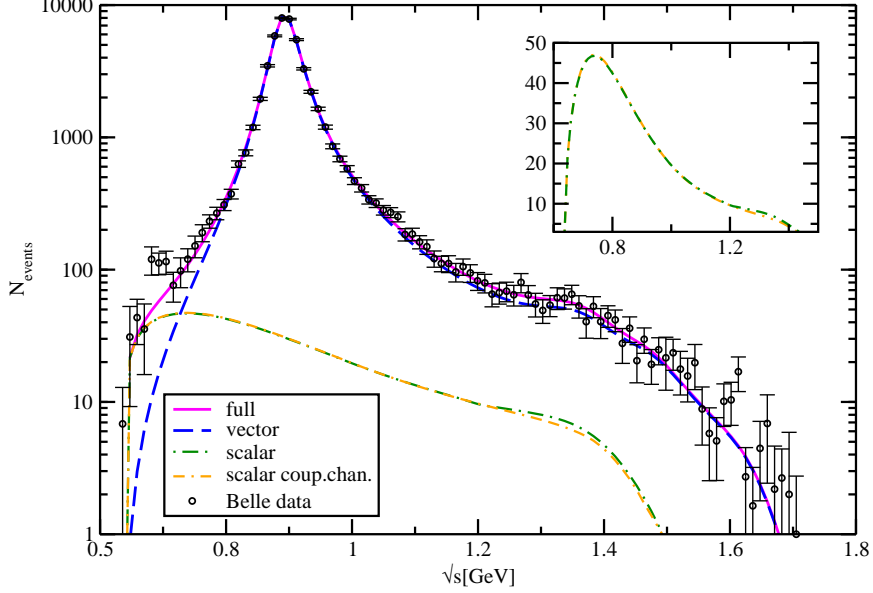


**Figure 3.** Spectrum of  $\tau \rightarrow K\pi\nu_\tau$ . The black circles are the Belle data [13]. The dot-dashed green and the dot-dashed-dashed orange line are the scalar form factor contribution from the dispersive analysis, Eq. (3.36) and the coupled channel model [27, 28] respectively. The dashed blue line represents the vector form factor contribution and the solid magenta line gives the full result. The inset shows the scalar form factor contribution on a linear scale.

gets  $h_1 = 1.04$  and  $h_2 = 1.35$ . The various terms contribute to the  $\chi^2$  as follows:

$$\chi^2 = 40.2 + 80.6 + 0.42 + 0.07 + 0.03 + 0.02 + 0.02 \quad (4.8)$$

where the first number corresponds to the sum of the three first terms ( $17.8 + 17.5 + 4.8$ ) in Eq. (4.7) i.e. it measures the quality of the fit of  $\pi K$  scattering. Note that in the Belle data, Fig. 3 there is a bump close to threshold given by three points, bins 6, 7 and 8 which cannot be accommodated within our parametrization (as well as others) and which does not seem to be present either in the BaBar data [12] or in the more recent Belle data [32]. This region contributes for 27 to the  $\chi^2$ , so that without these points the latter would be even better. In Fig. 3 is also shown the contribution to the spectrum from the scalar form factor and the vector one. The former clearly dominates in the threshold region, the vector one being responsible for the peak at the  $K^*(892)$  resonance. A measurement of the forward-backward asymmetry would be very useful to disentangle the two contributions [66], helping to get a better precision on the parameters of the two form factors. In Fig. 2 the phase of  $\pi K$  scattering in the  $P$  wave is identical to the one of the vector form factor

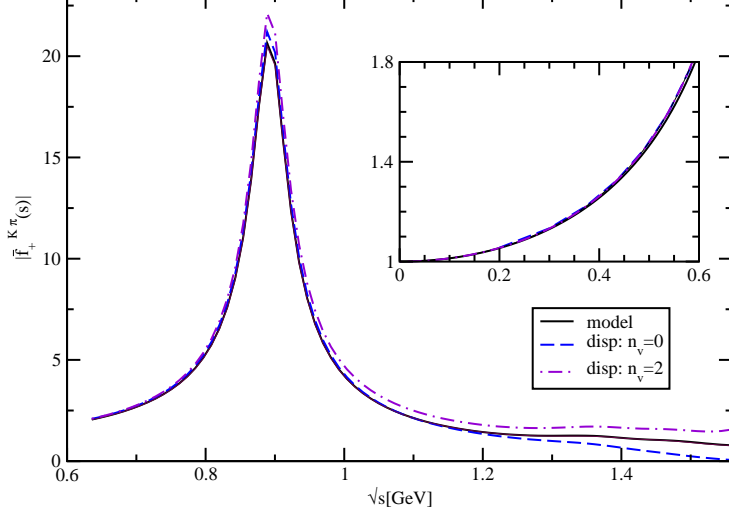


**Figure 4.** Modulus of the normalized vector form factor from the combined fit using the model parametrization of the vector form factor compared to the three subtracted dispersive analysis for two different values of the parameter  $n_v$ , Eq. (3.29) which parametrizes our ignorance of the phase at high energy. The solid black line corresponds to the result of the combined fit. The inset shows the result for low  $\sqrt{s}$ , the three curves in that region are almost undistinguishable.

in the elastic region as demanded by the Watson theorem and starts to deviate when the inelasticities set in.

The parameter  $\Lambda$ , Eq. (3.35) is set to 1.52 GeV in this fit. We have also performed a fit with  $\Lambda = 1.67$  GeV leading to similar results. Thus we refrain to show them here. Indeed the value where the inelasticities set in in the  $S$  wave is not very well known. A reasonable range of values is  $1.43 \text{ GeV} < \Lambda < 1.67 \text{ GeV}$  where the lower value is determined by the  $K^*$  resonance and the upper one is the energy where the phase of the amplitude is experimentally found to be different from the phase of the  $S$  matrix. Some discussion related to this can be found for example in [5, 16].

The values of our parameters in Table 1 are compatible with the estimated order of magnitudes discussed in section 4.1.  $a_0$  is at the upper end of the expected range leading to a rather small value of the decay constant in the chiral limit in favor of a paramagnetic suppression of the pion decay constant in the SU(3) chiral limit compared to the SU(2) one.  $g_V(1)/\sigma_V(1)$  are respectively somewhat smaller/larger than the ENJL predictions of Ref. [46].  $H_2(0)/f_+(0)$  compares well with its experimental value ( $f_+(0)$  is typically between 0.95 and 1), leading to a very small flavor breaking value  $a$ . Note also that integrating the spectrum obtained from the fit gives a value of  $I_k^\tau$  consistent with the value

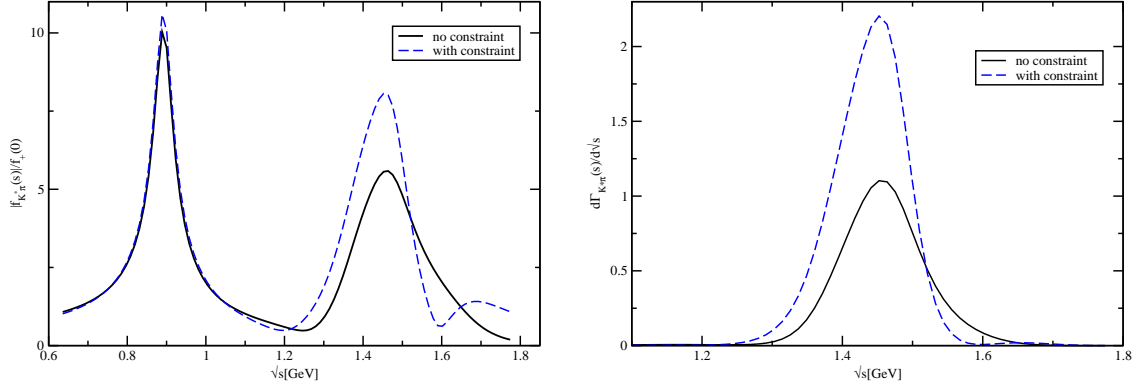


**Figure 5.** Modulus of the  $K^*\pi$  form factor divided by  $f_+(0)$  (left panel) and energy distribution of the decay width (right panel) as obtained in the combined fit. The black solid and blue dashed lines correspond to the fit without and with constraint on the curvature of the vector form factor respectively.

determined by the fitting procedure. We will discuss the results for  $f_+(0)|V_{us}|$  and  $\ln C$  below. Few remarks concerning the masses of the resonances are in order. First these are model dependent quantities. Second the data from LASS and FOCUS concern the neutral  $K^*$  while the published Belle analysis correspond to the charged  $K^*$ . Here we did not take into account isospin breaking however the PDG gives a difference of about 4 MeV between the two masses. Following [17, 18] we have thus calculated the complex pole positions  $s_R = m_R^2 - i\Gamma_R m_R$  [67] in the second Riemann sheet of the vector resonances which are much less model dependent. It also allows to determine the width of these resonances. One gets

$$\begin{aligned} M_{K^*(892)} &= (891.29 \pm 7.7) \text{ MeV} \quad , \quad \Gamma_{K^*(892)} = (46.26 \pm 5.01) \text{ MeV} \\ M_{K^*(1410)} &= (1370.65 \pm 35.93) \text{ MeV} \quad , \quad \Gamma_{K^*(1410)} = (164.93 \pm 34.56) \text{ MeV} \end{aligned} \quad (4.9)$$

As expected from the quality of the fit, the results for the  $K^*(892)$  are in agreement with LASS, Eq. (4.2) within the error bars while the central value of the mass is close to the PDG recommended value  $M_{K^*(892)} = 891.66 \pm 0.26$  MeV for the charged  $K^*$ . The width is somewhat too small though within the error bars, the PDG quotes for the charged  $K^*$ ,  $\Gamma_{K^*} = 50.8 \pm 0.9$  MeV. However as noted in [18] the PDG values are chiefly obtained from the parameters of Breit Wigner type expressions and thus need not to be exactly the same as determined from the pole position. This remark also holds for the  $K^*(1410)$  where the PDG gives  $M_{K^*(1410)} = 1414 \pm 15$  MeV and  $\Gamma_{K^*} = 232 \pm 21$  MeV.

In Fig. 4 is shown the result of the fit for the modulus of the normalized vector form factor. It increases from one at zero momentum transfer up to the  $K^*(890)$  resonance region where it shows a strong peak. The values of its slope and curvature are given in Table 2 and compared with results obtained from a quadratic fit to  $K_{\ell 3}$  data and various theoretical results from earlier works on  $\tau \rightarrow K\pi\nu_\tau$  decay. The slope is in good agreement and the

curvature even though compatible with most of the experimental results which are rather spread with large error bars, has a central value a bit small compared to the theoretical results. Also our results for the slope and curvature lie within the allowed domains obtained in [51, 75] within the method of unitarity bounds. The vector form factor is compared in Fig. 4 to the result of a dispersive analysis, Eqs. (3.27-3.29) for two values of the parameter  $n_v$ , corresponding to a very conservative estimate of our ignorance of the phase at high energy, using our result for the slope and the phase up to 1.6 GeV, while the curvature is determined from the sum rule, Eq. (3.39). The generated band is very small up to  $\sim 0.85$  GeV and broadens as the energy increases further. However the uncertainty from the high energy phase is not too large up to 1.6 GeV. Our form factor is compatible with the dispersive analysis for  $n_v \sim 0$ . Let us consider the sum rules. The RHS of the first one, Eq.(3.38) is  $(17.022 + 7.609 n_v) \times 10^{-3}$  where the first number corresponds to the integral from threshold to  $\Lambda = 1.6$  GeV while the second is the remaining contribution up to infinity taking the value  $\pi$  for the phase. As expected the latter contribution is sizeable leading in principle to a rather large uncertainty from the high energy region. For a not too large violation of the sum rule  $n_v$  should lie typically between 0.74 and 1.4. Clearly the second sum rule, Eq. (3.39) has a much smaller uncertainty from the high energy region, one gets from the RHS  $(5.556 + 0.579 n_v) \times 10^{-4}$  leading to a value of the curvature of the form factor using  $n_v$  in the range just given and taking into account the error on the slope,  $1.23 \times 10^{-4} < \lambda''_+ < 1.30 \times 10^{-4}$ . We will briefly come back on the issue of the size of  $\lambda''_+$  at the end of the section.

The modulus of the  $K^*\pi$  vector form factor is illustrated in the left panel of Fig. 5. It has two peaks of the same order of magnitude, one at the  $K^*(890)$  resonance which is of course much less pronounced than the analog peak in  $f_+(s)$  and the other one close to the second resonance  $K^*(1410)$ . This leads to the energy distribution of the decay width  $d\Gamma_{K^*\pi}(s)/d\sqrt{s}$ , Eq. (2.11) shown in the right panel of the same figure. It is consistent with the theoretical work [16]. Integrating this distribution gives the integrated rate  $R(\tau \rightarrow K^*(1410)\nu_\tau \rightarrow K\pi\pi\nu_\tau)$ . The result is shown in Table 2. The central value is smaller than the Aleph result, however, within the error bars which are rather large both for theory and experiment. Upcoming experiments on  $\tau \rightarrow K^*(1410)\nu_\tau \rightarrow K\pi\pi\nu_\tau$  will help constraining the parameters of the model further.

In Table 2 are also given the predicted values for the  $K\pi$  scattering length  $a_1^{1/2}$  and the branching ratio  $B_{K\pi}$ , Eq. (2.5).  $a_1^{1/2}$  turns out to be somewhat too large compared to various predictions, the last column giving some results from  $\chi$ PT,  $R\chi$ PT, Roy equations and  $\tau$  decay. Note however that there is a lack of constraints from the experimental data in the threshold region and that the same too large value was also obtained in a similar combined analysis [16] contrary to [18] where only the Belle spectrum was fitted.

Let us discuss the value of  $n_s$ , Eq. (4.7). As we have seen in section 3.4  $\ln C$  obeys a sum rule. Using our parametrization of the unknown phase, Eq. (3.35) one gets

$$n_s = \frac{1}{G_{as}} \left( \ln C - \frac{\Delta_{K\pi}}{\pi} \int_{s_{K\pi}}^{\Lambda} ds' \frac{\delta_0^{K\pi}(s')}{s'(s' - \Delta_{K\pi})} \right) = \frac{1}{0.10446} (0.2062 - 0.1336) = 0.696 \quad (4.10)$$

|                               |                   |                   |  |
|-------------------------------|-------------------|-------------------|--|
| $a_1^{1/2} \times 10 m_\pi^3$ | $0.249 \pm 0.011$ | $0.247 \pm 0.001$ | $0.16(3) \ 0.18, 0.18(3), 0.19(1), 0.17$   |
| $\lambda'_+ \times 10^3$      | $25.56 \pm 0.40$  | $25.58 \pm 0.09$  | $20.64(1.75), 25.6(1.8), 24.86(1.88), 24.80(1.56)$<br>$26.05^{+0.21}_{-0.58}, 25.20(33), 24.66(77), 25.49(36)$ |
| $\lambda''_+ \times 10^3$     | $1.11 \pm 0.08$   | $1.22 \pm 0.02$   | $3.20(69), 1.5(8), 1.11(74), 1.94(88)$<br>$1.29^{+0.01}_{-0.04}, 1.29(3), 1.20(2), 1.22(2)$                    |
| $B_{K\pi}[\%]$                | $0.414 \pm 0.008$ | $0.414 \pm 0.005$ | $0.404 \pm 0.02 \pm 0.013, 0.416 \pm 0.01 \pm 0.008$   |
| $R \times 10^3$               | $0.70 \pm 0.43$   | $1.23 \pm 0.05$   | $1.4^{+1.3}_{-0.9}$  |

**Table 2.** Prediction for the  $K\pi$  scattering length  $a_1^{1/2}$ , the slope and curvature of the vector form factor, the branching ratio and the integrated rate  $R(\tau \rightarrow K^*(1410)\nu_\tau \rightarrow K\pi\pi\nu_\tau)$ . The second and third column give respectively the results of the fit without and with the constraint on the curvature of the vector form factor. The last column summarizes also various theoretical predictions for  $a_1^{1/2}$ ,  $\lambda'_+$  and  $\lambda''_+$  as well as experimental results for the two latter quantities and the integrated rate. From left to right the numbers for  $a_1^{1/2}$  correspond to  $\chi$ PT at  $\mathcal{O}(p^4)$  [68] and at  $\mathcal{O}(p^6)$  [69], R $\chi$ PT at  $\mathcal{O}(p^4)$  [70], a Roy-Steiner dispersive analysis of  $\pi K$  scattering [56] and a  $\tau$  decay analysis [18]. The experimental numbers from  $K_{\ell 3}$  data (first line) for  $\lambda'_+$  and  $\lambda''_+$  are from left to right from KTeV [71], KLOE [8, 72], NA48 [7, 73] and ISTRA+ [74]. The theoretical numbers (second line) are from earlier works on  $\tau \rightarrow K\pi\nu_\tau$  without constraints from  $K_{\ell 3}$  [15]-[17] and with constraints [18]. The experimental results for  $B_{K\pi}$  are from [13, 33] respectively.

where  $G_{as}$  corresponds to the integral from  $\Lambda$  to infinity with the phase equal to  $\pi$ . The sum rule is satisfied for  $n_s = 0.696$ . We have allowed for some violation of the sum rule since  $G_{as}$  is not known, our fit leading to a 5% discrepancy. As discussed previously for the vector form factor the second sum rule, Eq. (3.41) has a much smaller uncertainty from the high energy region, one gets from the RHS of this equation,  $0.152 + 0.018 n_s$ . Thus with  $n_s$  as given from the fit the slope of the scalar form factor is  $\lambda_0 = 0.0144 \pm 0.0007$ .

The modulus of the normalized scalar form factor is depicted in Fig.6 for three different values of the parameter  $n_s$  keeping the value at the CT point fixed. These values gives a violation of the sum rules by 15% for  $n_s = 0.4$  and 30% for  $n_s = 1.25$ . The uncertainty due to the high energy phase is much larger than in the vector form factor case, fortunately the sum rules help reducing it sizeably. The form factor has a first small bump around the  $K^*(890)$  resonance and a second one around the  $K^*(1410)$  one, the latter being more or less pronounced depending on the value of  $n_s$ . This behaviour agrees with older calculations of the  $\pi K$  scalar form factor, see [27] as well as the recent work [29]. The  $\tau$  data combined with  $\pi K$  scattering plus constraints from the sum rules demand a somewhat stronger second bump compared to the first one which compares also very well with [57]. The behaviour of our form factor above  $\sim 1.25$  GeV is sensitive to the value of the parameter  $\Lambda$  as shown

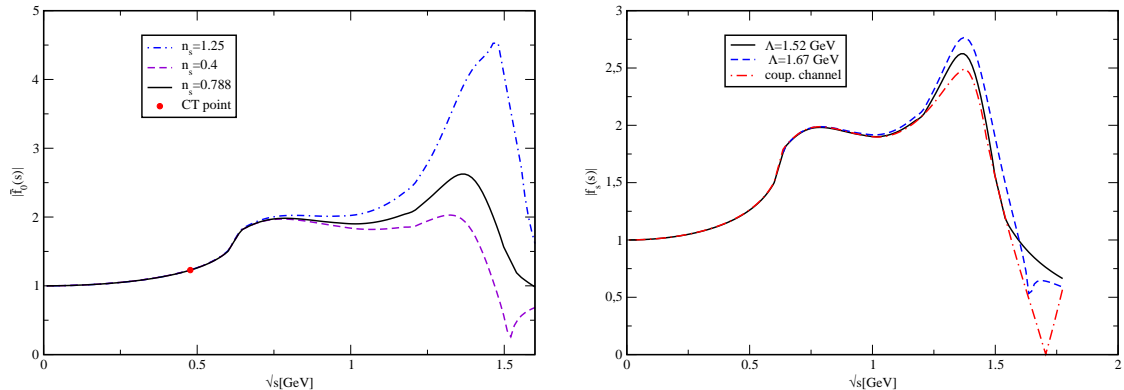


**Figure 6.** Left panel: modulus of the normalized scalar form factor for three different values of the parameter  $n_s$ , Eq. (3.35) which parametrizes our ignorance of the phase at high energy. The solid black line corresponds to the result of the combined fit. The Callan-Treiman (CT) point is shown by the red circle. Right panel: modulus of the normalized scalar form factor for two different values of the cut off  $\Lambda$ , Eq. (3.35) and from a fit to a coupled channel analysis [27, 28].

on Fig. 6. To compare further our model independent description of the scalar form factor we have repeated the combined fit <sup>6</sup> using a coupled channel dispersive analysis analogous to [27, 28] for describing this form factor. Indeed such a model has been extensively used in various works on  $\tau \rightarrow K\pi\nu_\tau$ . However in the line of what has been done here we do not fix the value of the scalar form factor at the CT point contrary to what is done in these works. We obtain very similar results for the fit parameters and thus refrain to present them here, let us just quote the value of  $\ln C = 0.2061 \pm 0.0086$ ,  $f_+(0)|V_{us}|$  being the same as in Table 1. The three form factors are compared in Fig. 6 while in Fig. 3 the scalar contributions to  $N_{\text{events}}$  obtained in the fit with  $\Lambda = 1.52$  GeV and with the coupled channel analysis are shown. The three form factors start to differ as one gets closer to the region where the inelasticities set in due to a different drop of the phase more or less abrupt which is then followed by a growth, see [5, 28, 52, 76].

Let us finally discuss the value of  $f_+(0)|V_{us}|$  obtained adding the constraint from  $K_{\ell 3}$  decays as explained below Eq. (4.7). It is compared in Fig. 7 to several values determined from five  $K_{\ell 3}$  decay modes, see Ref. [3] for more details. Assuming the SM couplings and using  $V_{ud} = 0.97425(22)$  from a recent survey [2] one gets

$$f_+(0) = 0.959(6), \quad (4.11)$$

which is within the error band of the lattice averaging from FLAG-1 [77],  $f_+(0) = 0.956(8)$ . It is also compatible with the results from the updated version [78]. There, according to the FLAG quality criteria, the results of two collaborations are given as the new averages:  $f_+(0) = 0.9667(23)(33)$  from MILC ( $N_f = 2 + 1$ ) [79] and  $f_+(0) = 0.9560(57)(62)$  from ETM09A ( $N_f = 2$ ) [80].

<sup>6</sup>I would like to thank B. Moussallam for providing me with his fortran code.



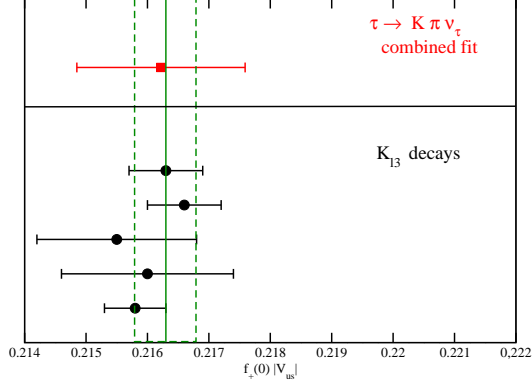


**Figure 7.** Determination of  $f_+(0)|V_{us}|$  from semileptonic kaon decays (on the lower portion) and from the combined fit (upper portion). The band corresponds to the average of the semileptonic data from [3].

One can now compare the result for  $\ln C$  from the fit with its expression from the Callan-Treiman theorem. Experimental information on the inclusive  $K_{\ell 2}$  and  $\pi_{\ell 2}$  decay rates and precise knowledge of the radiative corrections lead to [3]

$$F_K^+/F_\pi^+|V_{us}/V_{ud}| = 0.2758(5). \quad (4.12)$$

Assuming again the SM couplings and the value of  $f_+(0)$  as given by our fit, Eq. (4.11) one gets

$$\Delta_{CT} = (-1.29 \pm 1.28) \times 10^{-2}, \quad (4.13)$$

whose central value is somewhat larger than expected from  $\chi$ PT calculations. However considering the large error bar the value of  $\Delta_{CT}$  is compatible with the NLO  $\chi$ PT result in the isospin limit [47]  $(-0.35 \pm 0.8) \times 10^{-2}$  (the error is a conservative estimate of the higher order corrections), NNLO estimates with isospin breaking given in [36, 81], and chiral extrapolations to lattice data [62, 82]. Similarly for the form factor at the soft kaon analog point one gets

$$\bar{f}_0(-\Delta_{K\pi}) = 0.865 \pm 0.008, \quad \tilde{\Delta}_{CT} = (-0.972 \pm 0.941) \times 10^{-2}, \quad (4.14)$$

where  $\tilde{\Delta}_{CT}$  is defined by the following  $SU(3) \times SU(3)$  theorem

$$f_0(-\Delta_{K\pi}) = \frac{F_{\pi^+}}{F_{K^+}} + \tilde{\Delta}_{CT}. \quad (4.15)$$

As for  $\Delta_{CT}$  the error bars are large and the result is again compatible with  $\chi$ PT calculations and chiral extrapolation of the lattice data [62, 82]. In the former case one gets  $\tilde{\Delta}_{CT} = 0.03$  at NLO in the isospin limit [47], while at two loop order two low energy constants enter [83] leading to the following estimate  $-0.035 < \tilde{\Delta}_{CT} < 0.11$  [5]. Hence at present our results are compatible with the SM.

|                        | $\lambda''_+$ unconstr. | $\lambda''_+$ constr. |                         | $\lambda''_+$ unconstr. | $\lambda''_+$ constr. |
|------------------------|-------------------------|-----------------------|-------------------------|-------------------------|-----------------------|
| $\ln C$                | $0.2051 \pm 0.0088$     | $0.2043 \pm 0.0081$   | $f_+(0) V_{us} $        | $0.227 \pm 0.008$       | $0.230 \pm 0.002$     |
| $M_K$                  | $892.70 \pm 1.11$       | $891.62 \pm 0.18$     | $M_{K^*}$               | $1366.76 \pm 28.44$     | $1376.24 \pm 2.64$    |
| $\Gamma_K$             | $46.62 \pm 1.11$        | $46.21 \pm 1.97$      | $\Gamma_{K^*}$          | $155.72 \pm 39.68$      | $195.51 \pm 2.37$     |
| $\lambda' \times 10^3$ | $25.56 \pm 0.41$        | $25.59 \pm 0.05$      | $\lambda'' \times 10^3$ | $0.81 \pm 0.30$         | $1.22 \pm 0.02$       |
| $I_k^\tau$             | $0.444 \pm 0.029$       | $0.431 \pm 0.002$     | $R \times 10^3$         | $0.66 \pm 0.41$         | $1.24 \pm 0.04$       |
| $n_s$                  | $0.774 \pm 0.259$       | $0.758 \pm 0.204$     | $\chi^2$                | 119.89/128              | 118.58/128            |

**Table 3.** Results of two fits where  $f_+(0)|V_{us}|$  is left free and  $\lambda''$  is either constrained or not. The mass and width of the resonances are in MeV. For more details see text and Tables 1, 2.

#### 4.3.2 Role of the constraint on $f_+(0)|V_{us}|$ and of the curvature of $f_+(s)$ .

Before concluding let us discuss the role played by the constraint on  $f_+(0)|V_{us}|$  from  $K_{\ell 3}$  decays which we have included in our fit as well as the result on the curvature of  $f_+(s)$ .

In order to see the role played by the constraint on  $f_+(0)|V_{us}|$  (see Eq. (4.7) and discussion below) we have performed a similar fit without this constraint. The results are shown in Table 3. The  $\chi^2 \equiv \chi^2_{\text{noctfV}}$  is similar in the two cases, however the value of  $f_+(0)|V_{us}|$  is larger with a smaller uncertainty. Consequently the value of  $I_k^\tau$  is smaller, the value of  $B_{K\pi}$  being similar in the two fits due to the rather strong constraint from the new Belle result. Interestingly the central value of the curvature of the vector form factor is now much smaller leading to a 35% violation of the sum rule for  $n_v = 0$ . However the error bar is rather large.

We have thus performed a new fit constraining the value of  $\lambda''_+$  to be within the range given in [18], see Table 2, first leaving the constraint on  $f_+(0)|V_{us}|$ . The  $\chi^2$  has now one additional term

$$\chi^2 = \chi^2_{\text{noct}\lambda''} + \left( \frac{\lambda''_+ - 1.22}{0.02} \right)^2 \quad (4.16)$$

where  $\chi^2_{\text{noct}\lambda''}$  is the expression, Eq. (4.7). In this new fit we fixed the value of  $a_0$  since a larger value of the slope prefers a larger value of this parameter. Results are compared in the third columns of Table 1 with the fit without constraints on the curvature. The values of  $\ln C$ ,  $f_+(0)|V_{us}|$  and  $\Delta_{CT} = (-1.26 \pm 1.14) \times 10^{-2}$  are quite stable, the parameters mostly changed being the ones related to the  $K^*\pi$  channel. However due to the rather strong constraint we have imposed, the error bars are in most cases much smaller. The mass and width of the resonances are now:

$$\begin{aligned} M_{K^*(892)} &= (891.22 \pm 1.70) \text{ MeV} \quad , \quad \Gamma_{K^*(892)} = (46.26 \pm 1.99) \text{ MeV} \\ M_{K^*(1410)} &= (1379.84 \pm 23.59) \text{ MeV} \quad , \quad \Gamma_{K^*(1410)} = (179.35 \pm 36.42) \text{ MeV} \end{aligned} \quad (4.17)$$

to be compared with Eq. (4.9). Concerning the predictions, Table 2, similar results are obtained for most of the quantities except the curvature and the integrated rate  $R$  which is

now in better agreement with the central value of Aleph. This is due to a second bump in the modulus of the  $K^*\pi$  form factor which is now more pronounced than in the fit discussed in the previous subsection as seen in Fig. 5. As already stated a better measurement of the energy distribution of the decay width would be very useful to constrain the parameters of the fit.

For completeness we have finally repeated the fit without the constraint on  $f_+(0)|V_{us}|$ . The results are compared in Table 3 with the similar fit but without constraint on the curvature of the vector form factor.

The main conclusion from the studies performed on the role of the constraint on  $f_+(0)|V_{us}|$  is that given the experimental uncertainties on the spectrum the combined fits prefer a smaller value of  $I_k^\tau$  and consequently a larger value of  $f_+(0)|V_{us}|$ , the product of these two quantities being constrained by the branching ratio. However the values obtained are too large compared to the  $K_{\ell 3}$  ones. Clearly more precise data are needed to be able to determine  $f_+(0)|V_{us}|$  from  $\tau$  data alone.

## 5 Conclusion

The study performed here offers for the first time a direct extraction of  $f_+(0)|V_{us}|$  from  $\tau \rightarrow K\pi\nu_\tau$  decay. A model for the vector form factor valid in the region below  $\sqrt{s} \sim 1.65$  GeV is build from a N/D method. Using a simple dispersive approach for the scalar form factor (as well as a coupled channel method for comparison) a combined analysis of  $\tau \rightarrow K\pi\nu_\tau$  decay and  $\pi K$  scattering constrained by  $K_{\ell 3}$  and  $D_{\ell 4}$  data is performed. The coupled channel approach used here for the vector form factor allows to determine also the decay spectrum of  $\tau \rightarrow K^*(1410)\nu_\tau \rightarrow K\pi\pi\nu_\tau$  which is at present not very precisely measured. The result obtained for  $f_+(0)|V_{us}|$  is almost independent of the model used for the scalar form factor. The value of this form factor at the Callan-Treiman point as well as the soft kaon analog determined from the fit are compared to  $SU(N_f) \times SU(N_f)$  theorems with  $N_f = 2$  for the former and  $N_f = 3$  for the latter. At the level of accuracy of the data our results are compatible with the Standard Model. However, the forthcoming experiments will help reducing the uncertainty on  $f_+(0)|V_{us}|$  and  $\ln C$  allowing for a stringent test of the Standard Model. Indeed the errors in the  $\tau$  spectrum according to the expected sensitivity of a second generation B factory will be considerably reduced allowing for a determination of  $f_+(0)|V_{us}|$  from  $\tau$  data alone. Furthermore a measurement of the forward-backward asymmetry would be very useful to disentangle the scalar and vector form factors in the  $\tau$  spectrum. Finally this analysis should be refined to include the long distance electromagnetic and strong isospin breaking corrections and the effects from the unphysical cuts which have been neglected here once a much better precision of the data is reached.

## Acknowledgments

I thank B. Moussallam for sharing with me his very deep insights into the subject and S. Descotes-Genon and A. Le Yaouanc for enlightening discussions. I would also like to thank D. Boito for his participation at an early stage of the work and for very interesting

discussions and E. Passemar for some checks at an early stage of the work. I am also grateful to D. Boito, M. Döring, U.-G. Meißner, and B. Moussallam for careful reading of the manuscript and U.-G. Meißner for useful comments. This work is supported in part by the "EU I3HP Study of Strongly Interaction Matter" under the seventh Framework Program of the EU.

## References

- [1] J. Beringer *et al.* [Particle Data Group], Phys. Rev. D **86**, 010001 (2012).
- [2] J. C. Hardy and I. S. Towner, Phys. Rev. C **79** (2009) 055502 [arXiv:0812.1202 [nucl-ex]].
- [3] M. Antonelli *et al.* [FlaviaNet Working Group on Kaon Decays], Eur. Phys. J. **C69** (2010) 399-424 [arXiv:1005.2323 [hep-ph]].
- [4] V. Bernard, M. Oertel, E. Passemar and J. Stern, Phys. Lett. B **638**, 480 (2006) [hep-ph/0603202].
- [5] V. Bernard, M. Oertel, E. Passemar and J. Stern, Phys. Rev. D **80**, 034034 (2009) [arXiv:0903.1654 [hep-ph]].
- [6] M. Antonelli, D. M. Asner, D. A. Bauer, T. G. Becher, M. Beneke, A. J. Bevan, M. Blanke and C. Bloise *et al.*, Phys. Rept. **494** (2010) 197 [arXiv:0907.5386 [hep-ph]].
- [7] A. Lai *et al.* [NA48 Collaboration], Phys. Lett. B **647** (2007) 341 [hep-ex/0703002].
- [8] F. Ambrosino *et al.* [KLOE Collaboration], JHEP **0712** (2007) 105 [arXiv:0710.4470 [hep-ex]].
- [9] E. Abouzaid *et al.* [KTeV Collaboration], Phys. Rev. D **81** (2010) 052001 [arXiv:0912.1291 [hep-ex]].
- [10] M. Veltri, arXiv:1101.5031 [hep-ex]; M. Hita-Hochgesand for the NA48/2 Collaboration, talk at Moriond EW 12 conference 2012
- [11] M. Moulson, arXiv:1301.3046 [hep-ex].
- [12] S. Paramesvaran [BaBar Collaboration], proceedings of Meeting of DPF 2009, arXiv:0910.2884 [hep-ex].
- [13] D. Epifanov *et al.* [Belle Collaboration], Phys. Lett. B **654** (2007) 65 [arXiv:0706.2231 [hep-ex]].
- [14] M. Jamin, A. Pich and J. Portoles, Phys. Lett. B **640** (2006) 176 [hep-ph/0605096].
- [15] M. Jamin, A. Pich and J. Portoles, Phys. Lett. B **664** (2008) 78 [arXiv:0803.1786 [hep-ph]].
- [16] B. Moussallam, Eur. Phys. J. C **53**, 401 (2008) [arXiv:0710.0548 [hep-ph]].
- [17] D. R. Boito, R. Escribano and M. Jamin, Eur. Phys. J. C **59**, 821 (2009) [arXiv:0807.4883 [hep-ph]].
- [18] D. R. Boito, R. Escribano and M. Jamin, JHEP **1009**, 031 (2010) [arXiv:1007.1858 [hep-ph]].
- [19] D. Kimura, K. Y. Lee and T. Morozumi, Prog. Theor. Exp. Phys. **2013**, 053803 (2013) [arXiv:1201.1794 [hep-ph]].
- [20] V. Bernard, D. R. Boito and E. Passemar, Nucl. Phys. Proc. Suppl. **218** (2011) 140 [arXiv:1103.4855 [hep-ph]].

- [21] J. M. Link *et al.* [FOCUS Collaboration], Phys. Lett. B **621** (2005) 72 [hep-ex/0503043].
- [22] P. del Amo Sanchez *et al.* [BaBar Collaboration], Phys. Rev. D **83** (2011) 072001 [arXiv:1012.1810 [hep-ex]].
- [23] G. Bonvicini *et al.* [CLEO Collaboration], Phys. Rev. Lett. **88**, 111803 (2002) [hep-ex/0111095].
- [24] M. Bischofberger *et al.* [Belle Collaboration], Phys. Rev. Lett. **107** (2011) 131801 [arXiv:1101.0349 [hep-ex]].
- [25] J. P. Lees *et al.* [BaBar Collaboration], Phys. Rev. D **85** (2012) 031102 [Erratum-ibid. D **85** (2012) 099904] [arXiv:1109.1527 [hep-ex]].
- [26] A. Pich and J. Portoles, Phys. Rev. D **63**, 093005 (2001) [hep-ph/0101194].
- [27] M. Jamin, J. A. Oller and A. Pich, Nucl. Phys. B **622** (2002) 279 [arXiv:hep-ph/0110193];
- [28] B. El-Bennich, A. Furman, R. Kaminski, L. Lesniak, B. Loiseau and B. Moussallam, Phys. Rev. D **79**, 094005 (2009) [Erratum-ibid. D **83**, 039903 (2011)] [arXiv:0902.3645 [hep-ph]].
- [29] M. Döring, U.-G. Meißner and W. Wang, JHEP **1310** (2013) 011 [arXiv:1307.0947 [hep-ph]].
- [30] J. Erler, Rev. Mex. Fis. **50** (2004) 200 [arXiv:hep-ph/0211345];
- [31] M. Antonelli, V. Cirigliano, A. Lusiani and E. Passemar, JHEP **1310**, 070 (2013) [arXiv:1304.8134 [hep-ph]].
- [32] S. Ryu [Belle Collaboration], arXiv:1302.4565 [hep-ex].
- [33] S. Ryu *et al.* [Belle Collaboration], arXiv:1402.5213 [hep-ex].
- [34] B. Aubert *et al.* [BaBar Collaboration], Phys. Rev. D **76**, 051104 (2007) [arXiv:0707.2922 [hep-ex]]; B. Aubert *et al.* [BaBar Collaboration], Nucl. Phys. Proc. Suppl. **189**, 193 (2009) [arXiv:0808.1121 [hep-ex]].
- [35] W. J. Marciano and A. Sirlin, Phys. Rev. Lett. **71** (1993) 3629; A. Sirlin, Rev. Mod. Phys. **50** (1978) 573.
- [36] A. Kastner and H. Neufeld, Eur. Phys. J. C **57** (2008) 541 [arXiv:0805.2222 [hep-ph]].
- [37] V. Cirigliano, M. Giannotti and H. Neufeld, JHEP **0811** (2008) 006 [arXiv:0807.4507 [hep-ph]].
- [38] R. Barate *et al.* [ALEPH Collaboration], Eur. Phys. J. C **10**, 1 (1999) [hep-ex/9903014], R. Barate *et al.* [ALEPH Collaboration], Eur. Phys. J. C **11**, 599 (1999) [hep-ex/9903015].
- [39] J. A. Oller, E. Oset and A. Ramos, Prog. Part. Nucl. Phys. **45**, 157 (2000) [hep-ph/0002193].
- [40] J. A. Oller and E. Oset, Phys. Rev. D **60**, 074023 (1999) [hep-ph/9809337].
- [41] L. Castillejo, R.H. Dalitz and F.J. Dyson, Phys. Rev. **101**, 453 (1956).
- [42] G. Ecker, J. Gasser, A. Pich and E. de Rafael, Nucl. Phys. B **321** (1989) 311.
- [43] G. Ecker, J. Gasser, H. Leutwyler, A. Pich and E. de Rafael, Phys. Lett. B **223** (1989) 425.
- [44] J. Portoles, AIP Conf. Proc. **1322**, 178 (2010) [arXiv:1010.3360 [hep-ph]].
- [45] U.-G. Meißner, Phys. Rept. **161** (1988) 213.
- [46] J. Prades, Z. Phys. C **63** (1994) 491 [Erratum-ibid. C **11** (1999) 571] [hep-ph/9302246].
- [47] J. Gasser and H. Leutwyler, Nucl. Phys. B **250** (1985) 517.

- [48] U.-G. Meißner and J. A. Oller, Nucl. Phys. A **679**, 671 (2001) [arXiv:hep-ph/0005253].
- [49] T. A. Lahde and U.-G. Meißner, Phys. Rev. D **74**, 034021 (2006) [arXiv:hep-ph/0606133].
- [50] G. P. Lepage and S. J. Brodsky, Phys. Lett. B **87** (1979) 359.
- [51] G. Abbas, B. Ananthanarayan, I. Caprini and I. Sentitemsu Imsong, Phys. Rev. D **82**, 094018 (2010) [arXiv:1008.0925 [hep-ph]].
- [52] J. A. Oller and L. Roca, Phys. Lett. B **651**, 139 (2007) [arXiv:0704.0039 [hep-ph]].
- [53] D. Aston, N. Awaji, T. Bienz, F. Bird, J. D’Amore, W. M. Dunwoodie, R. Endorf and K. Fujii *et al.*, Nucl. Phys. B **296**, 493 (1988).
- [54] P. Estabrooks, R. K. Carnegie, A. D. Martin, W. M. Dunwoodie, T. A. Lasinski and D. W. G. S. Leith, Nucl. Phys. B **133**, 490 (1978).
- [55] C. G. Callan and S. B. Treiman, Phys. Rev. Lett. **16** (1966) 153; R. F. Dashen and M. Weinstein, Phys. Rev. Lett. **22** (1969) 1337.
- [56] P. Buettiker, S. Descotes-Genon and B. Moussallam, Eur. Phys. J. C **33**, 409 (2004) [hep-ph/0310283].
- [57] M. Jamin, J. A. Oller and A. Pich, Phys. Rev. D **74** (2006) 074009 [hep-ph/0605095].
- [58] B. Moussallam, Eur. Phys. J. C **14**, 111 (2000) [arXiv:hep-ph/9909292] ; JHEP **0008**, 005 (2000) [arXiv:hep-ph/0005245].
- [59] S. Descotes-Genon, N. H. Fuchs, L. Girlanda and J. Stern, Eur. Phys. J. C **34**, 201 (2004) [arXiv:hep-ph/0311120].
- [60] S. Descotes-Genon, Eur. Phys. J. C **52**, 141 (2007) [arXiv:hep-ph/0703154].
- [61] S. Descotes-Genon and J. Stern, Phys. Lett. B **488**, 274 (2000) [arXiv:hep-ph/0007082].
- [62] V. Bernard, S. Descotes-Genon and G. Toucas, JHEP **1101**, 107 (2011) [arXiv:1009.5066 [hep-ph]] ; JHEP **1206**, 051 (2012) [arXiv:1203.0508 [hep-ph]]. ; arXiv:1209.4367 [hep-lat].
- [63] W. M. Dunwoodie, private communication
- [64] B. Moussallam, private communication
- [65] B. Ananthanarayan and K. Shivaraj, Phys. Lett. B **628**, 223 (2005) [hep-ph/0508116].
- [66] L. Beldjoudi and T. N. Truong, Phys. Lett. B **351** (1995) 357 [hep-ph/9411423].
- [67] R. Escribano, A. Gallegos, J. L. Lucio M, G. Moreno and J. Pestieau, Eur. Phys. J. C **28** (2003) 107 [hep-ph/0204338].
- [68] V. Bernard, N. Kaiser and U.-G. Meißner, Nucl. Phys. B **357**, 129 (1991).
- [69] J. Bijnens, P. Dhonte and P. Talavera, JHEP **0405**, 036 (2004) [hep-ph/0404150].
- [70] V. Bernard, N. Kaiser and U.-G. Meißner, Nucl. Phys. B **364**, 283 (1991)
- [71] T. Alexopoulos *et al.* [KTeV Collaboration], Phys. Rev. D **70**, 092007 (2004) [hep-ex/0406003].
- [72] F. Ambrosino *et al.* [KLOE Collaboration], Phys. Lett. B **636**, 166 (2006).
- [73] A. Lai *et al.* [NA48 Collaboration], Phys. Lett. B **604**, 1 (2004).
- [74] O. Yushchenko *et al.*, Phys. Lett. B **581**, 31 (2004); Phys. Lett. B **589**, 111 (2004).
- [75] I. Caprini and E. -M. Babalic, Rom. J. Phys. **55**, 920 (2010) [arXiv:1011.5023 [hep-ph]].

- [76] B. Ananthanarayan, I. Caprini, G. Colangelo, J. Gasser and H. Leutwyler, Phys. Lett. B **602**, 218 (2004) [hep-ph/0409222].
- [77] G. Colangelo, S. Dürr, A. Jüttner, L. Lellouch, H. Leutwyler, V. Lubicz, S. Necco and C. T. Sachrajda *et al.*, Eur. Phys. J. C **71**, 1695 (2011) [arXiv:1011.4408 [hep-lat]].
- [78] S. Aoki, Y. Aoki, C. Bernard, T. Blum, G. Colangelo, M. Della Morte, S. Dürr and A. X. E. Khadra *et al.*, arXiv:1310.8555 [hep-lat].
- [79] A. Bazavov, C. Bernard, C. M. Bouchard, C. DeTar, D. Du, A. X. El-Khadra, J. Foley and E. D. Freeland *et al.*, Phys. Rev. D **87**, 073012 (2013) [arXiv:1212.4993 [hep-lat]].
- [80] V. Lubicz *et al.* [ETM Collaboration], Phys. Rev. D **80**, 111502 (2009) [arXiv:0906.4728 [hep-lat]].
- [81] J. Bijnens and K. Ghorbani, arXiv:0711.0148 [hep-ph].
- [82] V. Bernard and E. Passemar, JHEP **1004**, 001 (2010) [arXiv:0912.3792 [hep-ph]].
- [83] J. Bijnens and P. Talavera, Nucl. Phys. B **669**, 341 (2003) [hep-ph/0303103].